ATM 1046

LSP EXPLOSIVE PACKAGES

FRAGMENTATION STUDY

Prepared by: G. B. Min
G. B. Min

Approved: D. L. Dewhirst
Don L. Dewhirst

Approved: John Zimmer
John Zimmer

ABSTRACT

The purpose of this ATM is to estimate from theoretical considerations the probability of fragments from an LSP explosive package striking the ALSEP Central Station. For the assumptions listed, this probability is calculated to be less than .068% (.00068).

TABLE OF CONTENTS

I. INTRODUCTION

The Lunar Seismic Profiling Experiment requires that Explosive Charges be detonated on the lunar surface early in the ALSEP lunar mission. Two factors of the lunar environment are its ultra-high vacuum (no air resistance or air drag) and its low gravitational field. Both of these factors contribute to an increased trajectory of fragments. Therefore there is legitimate concern that fragments and debris from detonating an Explosive Package might strike and cause damage to the ALSEP Central Station. The purpose of this study is to determine the probability of fragmentation damage to the ALSEP Central Station.

One parameter of great importance in this study is the initial velocity of fragments ejected by the explosion. One method for obtaining the initial velocity is to assume that all of the explosive energy is converted into the kinetic energy of the fragments. Because much of the explosive energy goes into the blast wave and into the fracture energy of the case materials, this method establishes an upper bound to the initial velocity. Another method for obtaining the initial velocity is by reference to empirical data. Reference 1, the SRI report, presents test data that establishes a velocity range from 200 to 600 meters/second. The probability calculations presented in this study are based on kinetic energy considerations up to a limit of 600 meters/second.

The striking probability is considered as a compound probability of two conditional events. These events are associated with the number of fragments and their probability of hitting the target. Due to the irregular package configuration, the number of fragments and their break-up pattern are difficult to predict. Therefore a distribution curve similar to the chi-square distribution is assumed for convenience of calculation. The second event involves the trajectory. Since the ALSEP Central Station has a honeycomb panel on its top as a protective shield, the most probable damage would be from fragment penetration of the side curtains which are made of soft materials, such as mylar, silk mesh and Kapton. Therefore the damage criterion is based on the probability of striking the vertical sides of the Central Station, rather than on impacting its top surface.

If the prototype model field tests provide information about fragment sizes, numbers and break-up pattern, the collected data can be used to modify the curve assumed in the study for the first probability event.

II ENERGY DISTRIBUTION

The purpose of this chapter is to determine how the explosive energy might be distributed between blast wave energy and the kinetic energy of the fragments. The equations of this chapter are included for the sake of completeness. Because we will assume that the total energy of the explosive is converted into kinetic energy of fragments, the reader may omit a thorough understanding of this chapter.

The distribution of energy in a high explosive during explosion is highly complex. Three types of energy predominate:

1) E_F, Kinetic energy of the fragments.

2) E_2, Energy retained by the hot gases of the explosive

3) E_3, Energy contained within the region bounded by the blast wave front.

The sum of energies $E_2 + E_3$ is the energy associated with the blast wave itself. If we define $E_B = E_2 + E_3$, then:

$$E_T = E_F + E_B \qquad \text{(II-1)}$$

where E_T is the total energy released by the explosive. This expression separates the energy into two major categories: energy due to fragments and the kinetic and potential energy of the spherical blast wave. A wave of finite amplitude has the following relationship between pressure and velocity:

$$u = \frac{2a}{\gamma - 1}\left\{\left(\frac{p}{p_o}\right)^{(\gamma-1)/2\gamma} - 1\right\} \qquad \text{(II-2)}$$

where p_o = standard pressures, usually atmospheric

γ = ratio of specific heats (=1.405 on earth)
p = pressure
a =velocity of sound in undisturbed atmosphere
u = velocity of wave in air

Then the kinetic energy per unit mass can be expressed as a function of the pressure change:

$$\text{K.E.} = -/2\, u^2 = \frac{2a^2}{(\gamma-1)^2}\left\{ y^{(\gamma-1)/\gamma} - 2y^{(\gamma-1)/2\gamma} + 1\right\} \qquad \text{(II-3)}$$

where y = p/po.

The potential energy per unit mass is $\int (p/po)\, d(1/\rho)$ which, in view of the adiabatic relationship, $p/po = (\rho/\rho o)^{\gamma}$, is

$$P.E. = a^2 \{\frac{1}{\gamma(\gamma-1)} y^{(\gamma-1)/\gamma} + 1/\gamma\, y^{-1/\gamma} - 1/(\gamma-1)\} \qquad \text{(II-4)}$$

so that

$$E_B = P.E. + K.E. = a^2\{\frac{3\gamma-1}{\gamma/(\gamma-1)^2} y^{(\gamma-1)/\gamma}$$

$$+ \frac{1}{\gamma} y^{-1/\gamma} - \frac{4}{(\gamma-1)^2} y^{(\gamma-1)/2\gamma} + \frac{3-\gamma}{(\gamma-1)^2}\} \qquad \text{(II-5)}$$

The total energy of a complete spherical wave (per unit mass) is

$$4\pi \int_{r_1}^{r_0} E_B\, \rho\, r^2\, dr \qquad \text{(II-6)}$$

where r_0 and r_1 are the outer and inner limits of the wave.

Equation (II-6) provides a basis for calculating blast wave energies. However, in this study, we will set E_B equal to zero. This assumption provides conservative estimates of fragment velocities. That is, the velocities calculated in Chapter VI will neglect the blast wave component of energy and will therefore be upper bounds to the actual fragment velocities.

III. EQUATIONS OF MOTION

The purpose of this chapter is to determine from theoretical considerations the most probable velocity vector for fragments of the case following detonation.

Except for the six-pound charge, the explosive charges are of cylindrical shape with roughly equal dimensions between diameter and height. The housing of EP is of rectangular shape. Eccofoam of 3 lbs/ft^3 density is filled between the space of the rectangular wall and cylindrical charge. When the explosive is detonated at one end, the detonation wave moves down the case leaving the expanding case in its wake. The rectangular case is assumed to deform into a circular shape which is theoretically investigated by Reference 2. The gas pressure which acts on the foam and the case has both radial (expansion) and longitudinal (extrusion) components of velocity. The expanding gas gives kinetic energy to different parts of the case at different times.

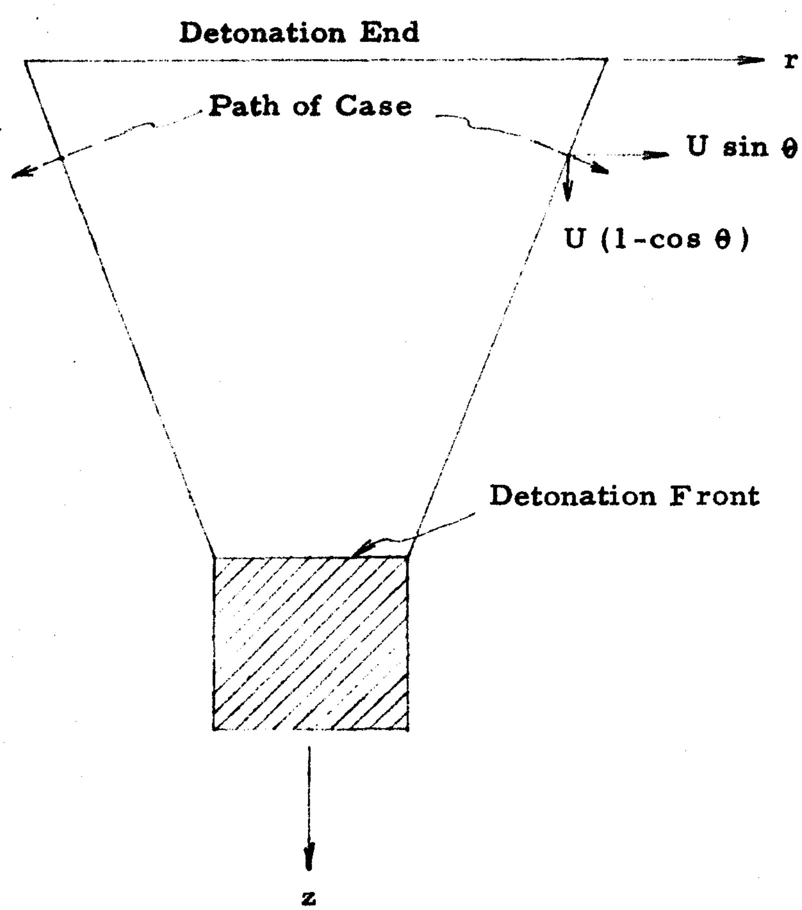

Based on the derivation of Reference 2, the equations of motion are presented as follows:

The equation of motion of the case is

$$\frac{MU^2}{2\pi r} \quad \frac{d^2 r}{dz^2} = p \qquad \text{(III-1)}$$

The equation of motion of the gas is

$$2 \int_{\rho_o}^{\rho_1} \frac{dp}{\rho} = u^2 - \frac{U^2}{\mu^2} \qquad \text{(III-2)}$$

And the equation of continuity is

$$u\rho r^2 = U\rho_o r_o^2 \qquad \text{(III-3)}$$

where

U = the velocity of the detonation wave

M = the mass of the case per unit length

r = expanding radius

p = gas pressure

z = distance measured along the axis

r_o = the external radius of charge before explosion

ρ_1 = density after detonating

ρ_o = density before detonating

u = the velocity of the gas

Equations (1), (2), (3), together with the adiabatic equation of state connecting p and ρ in the expanding gases, suffice to determine all the quantities concerned. By defining θ as the angle between an axial section of the case and the axis at distance z from the detonation front, the relationship is established (Ref 2) by using Eqs. (1), (2) and (3)

$$\tan^2\theta = \frac{2}{\alpha U} \left(\frac{p}{u\rho} + u - U \right) \qquad \text{(III-4)}$$

where

$$\alpha = \frac{M}{m} = \frac{\text{weight of case}}{\text{weight of explosive}} \qquad \text{(III-5)}$$

and U is determined by numerical integration of (2) using the p, ρ relationship.

The case is at rest until the detonation wave reaches it. Afterwards it moves with velocity whose components are $U(1-\cos\theta)$ forward in the direction of the detonation front and $U\sin\theta$ perpendicular to the axis. Combining these two components gives the velocity of the case:

$$v = U\sqrt{(1-\cos\theta)^2 + \sin^2\theta} = 2U\sin\frac{\theta}{2} \qquad \text{(III-6)}$$

If we equate the total explosive energy to the kinetic energy of the fragments as discussed in Chapter 2, we obtain from equation (III 6) and the trigonometric identity, $\sin^2\frac{\theta}{2} = \frac{1}{2}(1-\cos\theta)$:

$$E_T = E_F = \frac{1}{2}Mv^2 = MU^2(1-\cos\theta) \qquad \text{(III-7)}$$

Equation (III-7) can be solved for θ, if the magnitude of the explosive charge is known.

For small values of the angle θ, equation (III-6) can be simplified to the following form:

$$v \approx 2U\left(\frac{\theta}{2}\right) = U\theta \qquad \text{(III-8)}$$

IV. FRAGMENT TRAJECTORY

The motion of a particle in a uniform gravitational field is available in many testbooks. In order to fit this study, a modified set of the equations of the motion is derived.

The break-up pattern of the explosive package is more complex than predicted by the theory of Chapter 3. Much of the complication comes from the electronic instrument sitting on the top of the explosive. Although the fragment pattern during explosion is very complicated, two different approaches will be studied. The first approach is to consider a homogeneous fracturing such that all fragments are of equal size. Secondly nonuniform fragments will be assumed based on the package components. The following assumptions are made:

1. Since the air pressure and density on the lunar surface are 10^{-13} times that of the Earths surface, it is possible to neglect the air resistance.

2. When the explosion occurs, the fragments fly out radially from the explosion center, each with the same speed. For convenience, the trajectories in a plane bounded between θ° to 90° (θ defined in previous section) are considered. The resulting flight trajectories are described in the following figure.

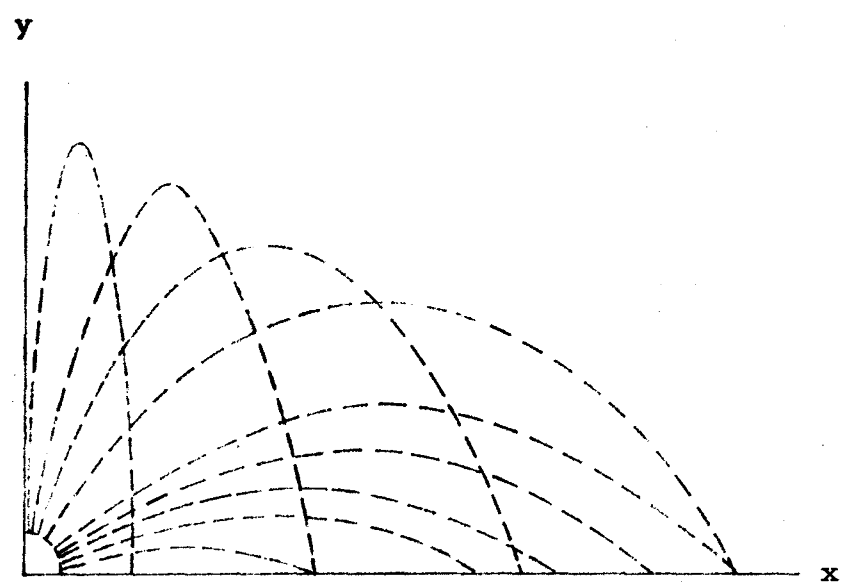

Based on the above assumptions, the motion of fragments in a uniform gravitation field can be derived as follows. Let the x y plane be the plane of motion with y axis directed vertically upward. Assume for convenience that the particle is located at the origin O at time t = O and is moving with velocity v_o at an angle ϕ with the horizontal. The initial velocity components are

$$v_x(0) = v_o \cos \phi \qquad \text{(IV-1)}$$

$$v_y(0) = v_o \sin \phi \qquad \text{(IV-2)}$$

with the acceleration components

$$a_x = o \qquad \text{(IV-3)}$$

$$a_y = -g \qquad \text{(IV-4)}$$

where g is the lunar gravity

Since the motions in the x and y directions are independent, the velocity and displacement components are

$$v_x = v_o \cos \phi \qquad \text{(IV-5)}$$

$$v_y = v_o \sin \phi - gt \qquad \text{(IV-6)}$$

$$x = v_o t \cos \phi \qquad \text{(IV-7)}$$

$$y = v_o t \sin \phi - 1/2\, g\, t^2 \qquad \text{(IV-8)}$$

Solving equation (IV-7) for t and substituting into equation (IV-8) gives:

$$y = x \tan \phi - \frac{g\, x^2}{2 v_o^2 \cos^2 \phi} \qquad \text{(IV-9)}$$

which is the equation for a parabolic trajectory. It is desired to arrange Eqtn (IV-9) to express the initial flight path angle ϕ in terms of any co-ordinates x, y through which a fragment may pass. Using the trigonometric identity

$$\frac{1}{\cos^2 \phi} = \sec^2 \phi = 1 + \tan^2 \phi \qquad \text{(IV-10)}$$

and rearranging the terms of Eqtn (IV-9), we have:

$$\tan^2\phi - \frac{2\,v_o^2}{gx}\tan\phi + \frac{2v_o^2}{gx^2} + 1 = 0 \quad \text{(IV-11)}$$

There are two rcots of this quadratic equation in tan ϕ, corresponsing to the low and high flight angles ϕ_1 and ϕ_2. Complex roots result for the case where the point is out of range. The roots are expressed as

$$\tan\phi = \frac{v_o^2}{gx} \pm \left\{\left(\frac{v_o^2}{gx}\right)^2 - \left(\frac{2v_o^2 y}{gx^2} + 1\right)\right\}^{1/2} \qquad \text{(IV-12)}$$

Having known values of y (the height of the central station), x (the distance between the explosive package and the central station), and v_o (the initial fragment velocity), Eqtn (IV-12) provides the desired angles ϕ, ϕ'.

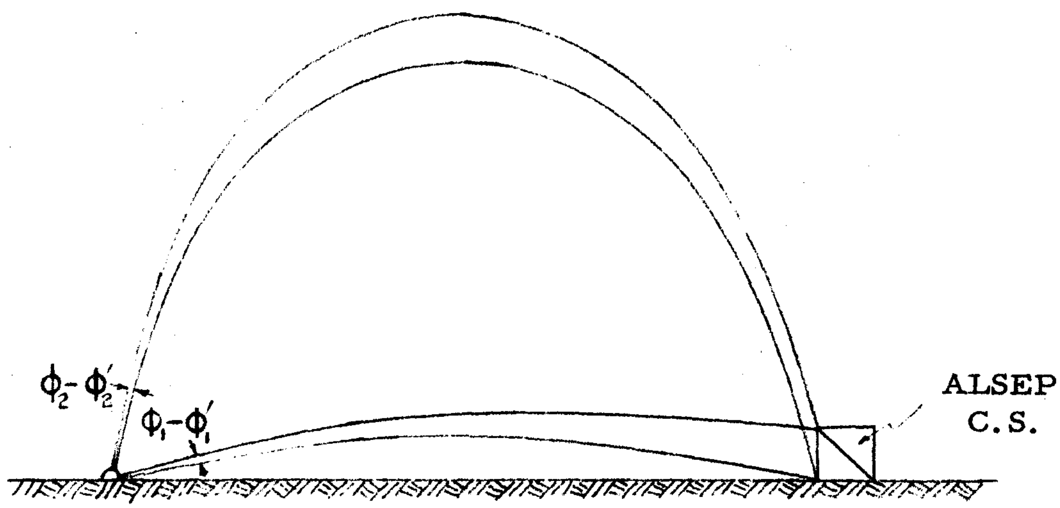

Eqtn (IV-12) can be applied to soil dust particles as well as explosive fragments. The volume of soil cratering can be estimated using Olsen's Formula:

$$V = 0.4\,Q^{8/7} \qquad \text{(IV-13)}$$

where V = volume in cubic ft, and Q = weight of exploding charge in pounds. See Ref 6. However this formula is quite conservative. Much of the debris cratered from below the explosive charge falls vertically back into the crater partially refilling it as shown in Figure 1. For the purposes of this study, we neglect the effects of these soil dust particles relative to the explosive fragments.

V. PROBABILITY DISTRIBUTION

Based on the assumptions stated in chapter 1, there are two events (X_1, X_2) influencing the determination of fragmentation probability. The first one deals with the probability associated with the number (X_1) of fragments produced. This probability curve can be determined through field test results. A probability curve using the chi-square distribution shown is assumed. The peak of the curve is based on consideration of mean value of non-uniform fragmentation, the tail of the curve on consideration of uniform fragmentation.

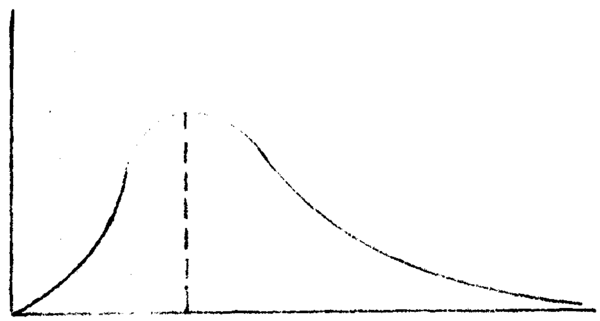

Its density is in the form:

$$p(\bar{x}) = \frac{1}{2^{\bar{m}/2}\Gamma(\bar{m}/2)} \bar{x}^{\bar{m}/2-1} e^{-\bar{x}/2} \qquad \bar{x}>0 \qquad \text{(V-1)}$$

where $\bar{x} = \frac{x_1}{n}$ (x_1: number of fragments; n: mean value of number of fragments)

$\bar{m}$ = degree of freedom = 4

$\Gamma(s)$ = gamma function = $\int_0^\infty z^{s-1} e^{-z} dz$

$\Gamma(4/2) = \Gamma(2) = 1 \cdot \Gamma(1) = 0! = 1$

$$\therefore p(\bar{x}) = 1/4\, \bar{x} e^{-\bar{x}/2} \qquad \text{(V-2)}$$

$$p(x_1) = \int_{x_1}^\infty p(\bar{x})\, d\bar{x}$$

The second event considers the striking probability of a known fragment number with velocity and location of target as its independent variables. By using the results of the range of striking angles in the previous section, this probability event can be expressed as follows:

$$p(x_2) = p(x_2|x_1) = N \cdot \frac{[(\phi_1 - \phi_1') + (\phi_2 - \phi_2')]}{2\pi} \cdot \frac{3.54\ (.3048)}{2\pi x} \qquad \text{(V-3)}$$

where X is the distance between the EP and the central station, and N is the number of fragments. The value of 3.54 feet comes from the maximum exposure range of side curtains perpendicular to the fragment path shown below.

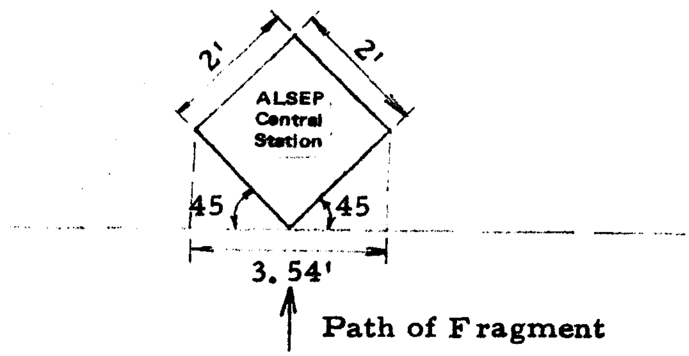

Now the compound probability can be calculated as follows:

$$p(x_1, x_2) = p(x_1)\, p(x_2|x_1) \qquad \text{(V-4)}$$

or

$$p(x_1, x_2) = p(x_2) \int_{x_1}^{\infty} p(\bar{x})\, a\bar{x} \qquad \text{(V-5)}$$

VI. SAMPLE NUMERICAL CALCULATIONS

A detailed description for the 1/8 lb charge explosive package at 125 meters distance is presented, step by step, as follows:

1. Weight of charge = .125#

   Weight of Housing Assy = .402# - .125# = .277#

   Weight of E & S/A Assy* = 2.286#

   Wt. of case = wt. of Housing Assy + wt. of E&S/A Assy = 2.286 + .277
   = 2.563#

2. Assume HNS charge energy $E = 1.5 \times 10^6$ ft-lb

   $$\therefore E_T = 1.5 \times 10^6 \times .125 = .1875 \times 10^6 \text{ ft-lb}$$

   $$= .1875 \times 10^6 \text{ ft-lb} \times \frac{.3048\text{M}}{\text{ft}} \times \frac{.4536\text{Kg}}{\text{lb}}$$

   $$= .0259234 \times 10^6 \text{ meter-Kg}$$

3. $$\alpha_1 = \frac{\text{wt. of case}}{\text{wt. of charge}} = 2.56/.125 = 20.5$$

   $$\alpha_2 = \frac{\text{wt. of housing}}{\text{wt. of charge}} = \frac{.277}{.125} = 2.216$$

4. From Del Mar Engineering Laboratories

   Gas front velocity, U = 7000 meters/sec.

5. Upper Bound of blast angle θ:

   $E_F = E_T$. From Eqtn (III-7):

   $$E_F = \alpha U^2 (1 - \cos\theta)$$

---

*Electronics and Safe/Arm Assembly

For α_1:

$$.02592 \times 10^6 = 20.5 \times (7000)^2 (1 - \cos \theta)$$

$$\cos \theta_1 = 1 - \frac{.02592}{20.5 \times 49} = 1 - .0000258 = .9999742$$

$$\therefore \quad \theta_1 = .41° = .41 \times \frac{3.1416}{180} = .00715587 \text{ radian}$$

For α_2:

$$\cos \theta_2 = 1 - \frac{.02592}{2.216 \times 49} = .99976129$$

$$\therefore \quad \theta_2 = 1.25^\circ = 1.25 \cdot \frac{3.1416}{180} = .02181667 \text{ radian}$$

6. **Theoretical fragment velocity, using eqtn (III-8):**

$$v_1 \cong U \times \theta_1 = 7000 \times .00715587 = 50.09 \text{ meter/sec}$$

$$v_2 \cong U \times \theta_2 = 7000 \times .021816 = 152.72 \text{ m/sec}$$

7. **Max. angle subtended by Central Station in plan view:**

$$\theta_H = \frac{3.54 \times .3048}{2\pi \times 125} = .0013738 \text{ radians}$$

8. **Vertical extended striking range from flight trajectory**

$$\theta_V = \text{(high striking angle)} + \text{(low striking angle)}$$

$$= (\phi_2 - \phi_2') + (\phi_1 - \phi_2')$$

Example (angle in radian)

Velocity (M/S)	ϕ_2	ϕ_2'	ϕ_1	ϕ_1'	θ_v
50	1.53025	1.53024	.0466513	.0405452	$.61165 \times 10^{-2}$
200	1.56826	1.56826	$.863626 \times 10^{-2}$	$.253295 \times 10^{-2}$	$.61033 \times 10^{-2}$
600	1.57051	1.57051	$.65917 \times 10^{-2}$	$.24414 \times 10^{-3}$	$.634756 \times 10^{-2}$

9. Conditional (independent) probability of strike based on fragment size

$$p(x_2) = p(x_2 \mid x_1) = N \cdot \frac{\theta_v}{\pi/2} \cdot \theta_H$$

Example: For V = 200 M/S

N	θ_v	θ_H	$p(x_2)$
2563	$.61033 \times 10^{-2}$	.0013738	.0136757
427	$.61033 \times 10^{-2}$	.0013738	.0022793
122	$.61033 \times 10^{-2}$	.0013738	.0006512

Refer to Table II for more results.

10. Probability of number of fragments based on the following assumed curve:

$$p(x_1) = \int_{x_1}^{\infty} p(\bar{x})\, dx$$

x_1	$p(x_1)$
2563	.05
427	.30
122	.95

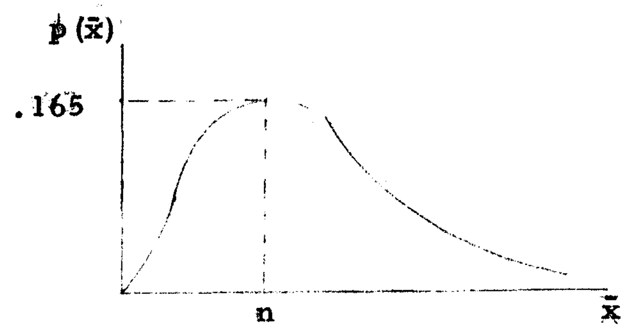

Refer to Table II for more results.

11. Resulting probability of striking ALSP Central Station

$p(x_1, x_2) = p(x_1)\, p(x_2 | x_1)$

Example: V = 200 M/S

x_1	$p(x_1)$	$p(x_2 \mid x_1)$	$p(x_1, x_2)$
2563	.05	.0136757	$.683786 \times 10^{-3}$
427	.30	.0022793	$.683786 \times 10^{-3}$
122	.95	.0006512	$.618664 \times 10^{-3}$

Refer to computer plots and Table II for more results.

12. Kinetic energy: This item may provide criteria of damage level.

$K.E. = 1/2\, m_f\, v^2$

where m_f is the mass of fragment. Use v = 200 M/S as sample.

Frag. wt. (lb)	K. E. (M-Kg)
.001	0.9251
.006	5.5505
.021	19.4268

Refer to computer plots for more results.

VII. CONCLUSIONS

The conclusions of this study are summarized in Tables I and II and Figures 2 through 16.

Table I presents the calculated values of upper bound velocities and blast angles for the assumption that the total explosive energy is converted into fragment kinetic energy. Two values of the mass ratio α are used, because the definition of this term is somewhat ambiguous for this situation. The results thus provide for any possible interpretation of α . The values of V_2 for the 3# and 6# charges are calculated by the theory as being greater than 7000 meter/sec. However, because fragment velocity cannot be greater than the gas front velocity, it is obvious that the assumptions used are conservative, and V_2 is therefore listed as 7000 M/S. Except for the 1/8 lb charge, all of the calculated velocities are greater than those given in Ref 1. Therefore, the results of Table I affect only the velocity range for the 1/8 lb charge of Table II.

Table II presents in column 7 the probability results based on the input parameters listed in columns 1 through 4. Column 5 lists the probability that the number of fragments is equal to or greater than the number listed in column 4. Column 6 lists the conditional probability $p(x_2 | x_1)$ described in Chapter V. The values in column 7 are the products of the corresponding numbers in columns 5 and 6. Note that, for example, for the 1/8 lb charge, a probability of .068% (i.e., .00068) is almost independent of the assumption regarding the number of fragments over the range considered.

Three distinct figures are presented for each charge mass. Figures 2, 5, 8, 11, and 14 present four curves each for kinetic energy as a function of particle (earth) weight, and velocity. These curves are included for the convenience of the readers, in case that a damage theory based on kinetic energy is used. Figures 3, 6, 9, 12 and 15 present conditional (or "independent") probabilities as functions of fragment initial velocities up to a limit of 600 meters/sec. Note that these probabilities are nearly independent of the velocity over the range considered. Finally, Figures 4, 7, 10, 13 and 16 present the striking probabilities as functions of fragment weight and velocity. Because of the small differences in some of the calculated probabilities, a few of the curves are virtually coincident, e.g., the 550 M/S and 600 M/S curves of Figure 4.

No damage criterion is given by this study. Such a criterion would probably be related to thermal control deterioration due to damage of the protective curtains.

VIII. REFERENCES

1. "Fragment Hazards Associated With the Active Seismic Experiment," by T. J. Ahrens and C. F. Allen, SRI Project FGU-6011 Report, May, 1967.

2. "Analysis of the Explosion of a Long Cylindrical Bomb Detonated at One End," by G. I. Taylor, Scientific Papers of G. I. Taylor, Vol. III, No. 30, Cambridge University Press (1963).

3. "Blast Impulse and Fragment Velocities from Cased Charge," by G. I. Taylor, Scientific Papers of G. I. Taylor, Vol. III, No. 40, Cambridge University Press (1963).

4. "The Dynamics of the Fragmentation Process for Spherical Shells Containing Explosives," by S. T. S. Al-Hassani and W. Johnson, Int. J. Mech. Sci., 1969, Vol. II, pp. 811-823.

5. "Theoretical Blast-Wave Curves for Cast TNT," by John G. Kirkwood and S. R. Brinkley, Jr., OSRD Report No. 5481.

6. Explosions: Their Anatomy and Destructiveness, by Clark S. Robinson, McGraw-Hill, 1946.

TABLE I UPPER BOUND VELOCITIES

(1) Charge Wt. & Distance	(2) Wt. of Housing (lb)	(3) Wt. of E & S/A (lb)	(4) Wt. of Case Col. (2)+Col. (3) (lb)	(5) Total Energy 10^6 (ft-lb)	(6) $\alpha_1 = \frac{\text{Col. (4)}}{\text{Col. (1)}}$	(7) $\alpha_2 = \frac{\text{Col. (2)}}{\text{Col. (1)}}$	(8) θ_1 (Radian)	(9) θ_2 (Radian)	(10) v_1 (m/s)	(11) v_2 (m/s)
							Using $E_F = E_T$ as Upper Bound			
1/8# *@ 125^m	.277	2.286	2.563	.1875	20.5	2.216	.007156	.02182	50	153
1/4# @ 250^m	.275	2.286	2.561	.375	10.244	1.1	.03875	.11807	271.25	826.49
1/2# @ 500^m	.410	2.286	2.696	.75	5.392	0.82	.075398	.20769	527.79	1453.8
1# @ 1000^m	.451	2.286	2.737	1.5	2.737	0.451	.14974	.3705	1048.2	2593.5
3# @ 3.5^km	.525	2.286	2.811	4.5	0.937	0.175	.4465	1.0756	3125.5	7000
6# @ 3.5^km	.528	2.286	2.814	9.0	0.469	.088	.9168	1.5708	6417.6	7000

(8), (9) = $\theta_i = \cos^{-1}\left(1 - \frac{E_T}{\alpha_i U^2}\right) = \cos^{-1}\left(1 - \frac{\text{Col. (5)}}{\alpha_i U^2}\right)$ (10), (11) = $v_i = U\theta_i$ U = 7000 m/s

* Actual planned minimum distance is 500 feet. 125 meters or 410 feet is used as minimum distance to assure conservative probability.

TABLE II STRIKING PROBABILITIES OF EXPLOSIVE PACKAGES

(1) Charge Wt. & Distance	(2) Velocity Range (meters/sec)	(3) Frag. Size (#)	(4) No. of Frag.	(5) $p(x_1)$ Chance	(6) Cond. $p(x_2/x_1)$ (%)	(7) Prob. $p = p(x_1) \times p(x_2/x_1)$ (%)
1/8#	50~600	.001	2563	.05	1.4	.068
@		.003	854	.15	.45	.068
125^m		.006	427	.30	.23	.068
		.009	285	.45	.15	.068
		.015	171	.75	.091	.068
		.021	122	.95	.065	.062
1/4#	200~600	.001	2561	.05	.343	.0172
@		.003	854	.15	.114	.0172
250^m		.006	440	.30	.057	.0172
		.009	285	.45	.038	.0171
		.015	171	.75	.023	.017
		.021	122	.95	.016	.015
1/2#	200~600	.001	2696	.05	.09	.0045
@		.003	895	.15	.03	.0045
500^m		.006	450	.30	.015	.0045
		.009	300	.45	.01	.0045
		.015	180	.75	.006	.0045
		.021	128	.95	.0043	.0041
1#	200~600	.001	2737	.065	.0228	.00148
@		.003	912	.135	.0076	.00103
1000^m		.009	304	.48	.0025	.0012
3#	200~600	.001	2811	.10	.0019	.000190
@		.003	938	.18	.0006	.000108
3.5^{km}		.006	409	.32	.0003	.000090
		.009	313	.48	.0002	.00096
		.015	188	.77	.00013	.0001
6#	200~600	.001	2814	.15	.0019	.00029
@		.003	938	.20	.0006	.00013
3.5^{km}		.006	469	.35	.0003	.00011
		.009	313	.50	.0002	.00011
		.015	188	.80	.00013	.0001

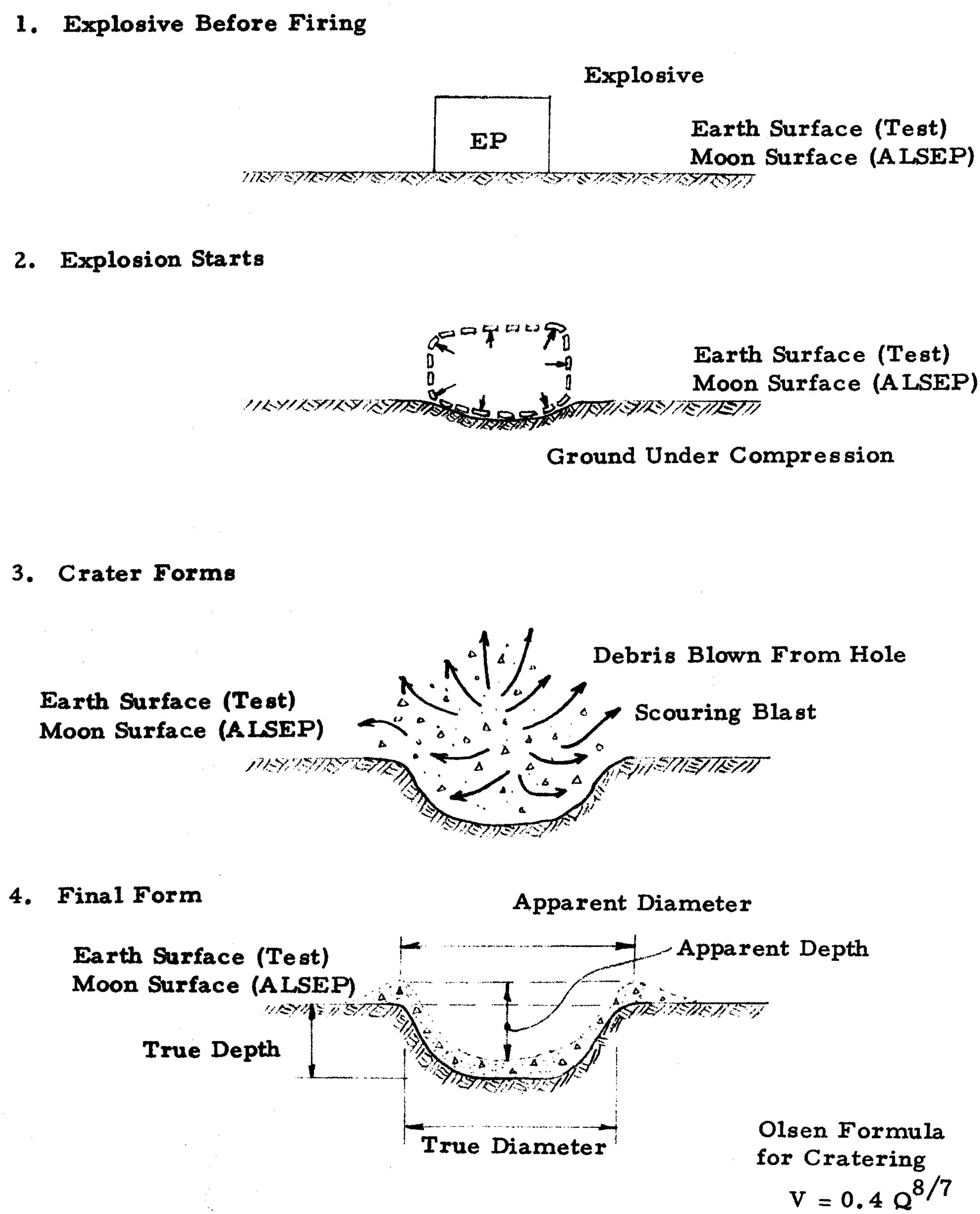

Figure 1 Diagram of EP Explosion

BENDIX AEROSPACE SYSTEMS DIVISION-FRAGMENTATION STUDY

CHARGE WT. (#) =0.125 CASE WT. (#) =2.563 DISTANCE (METERS) =125

□ FRAGMENT WT. (#) =0.001 ○ FRAGMENT WT. (#) =0.003 △ FRAGMENT WT. (#) =0.006
+ FRAGMENT WT. (#) =0.009

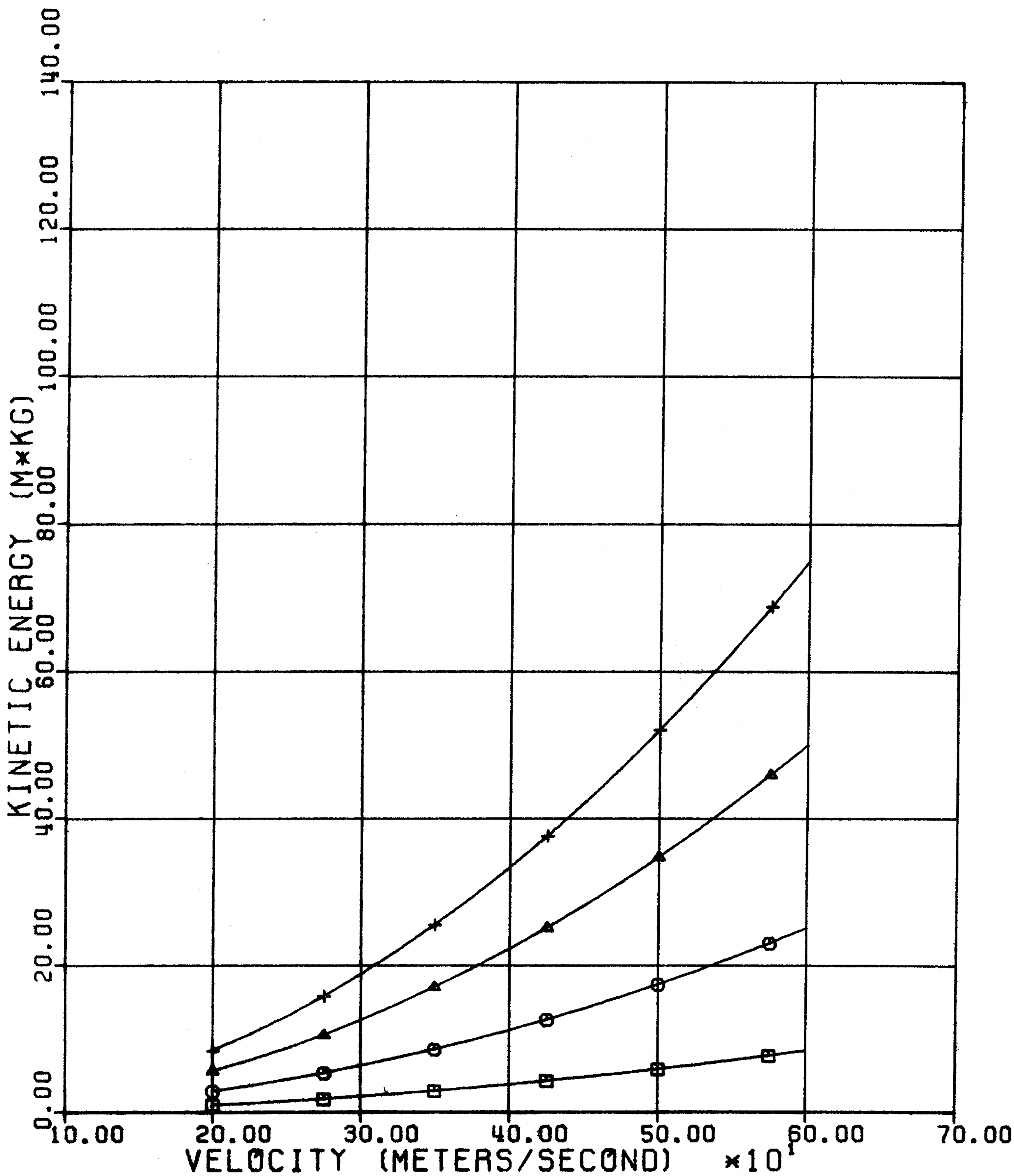

FIGURE 2 FRAGMENT K.E. VS. VELOCITY

BENDIX AEROSPACE SYSTEMS DIVISION-FRAGMENTATION STUDY

CHARGE WT. (#) =0.125 CASE WT. (#) =2.563 DISTANCE (METERS) =125

□ FRAGMENT WT. (#) =0.001 ○ FRAGMENT WT. (#) =0.003 △ FRAGMENT WT. (#) =0.006
+ FRAGMENT WT. (#) =0.009

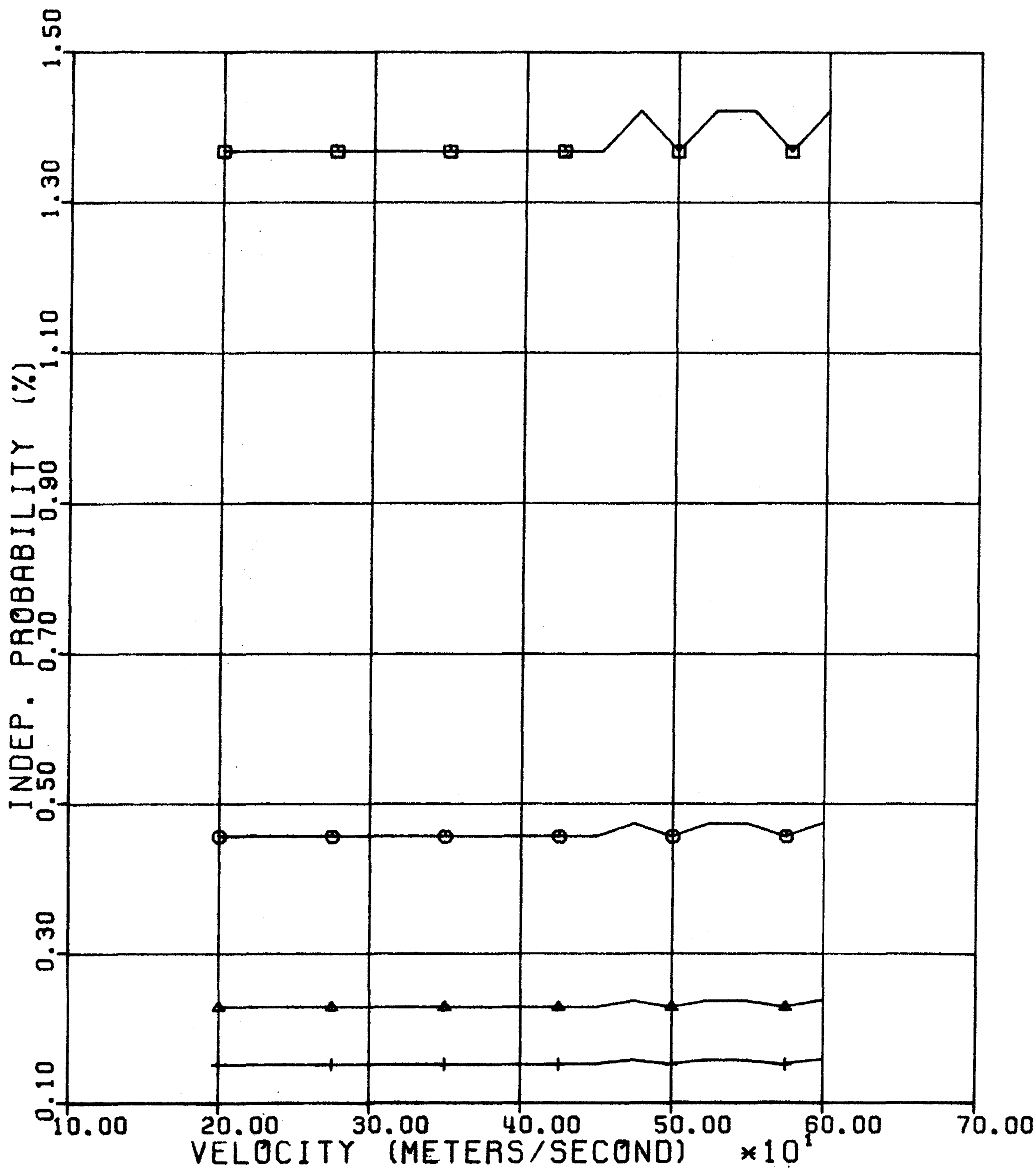

FIGURE 3 INDEPENDENT PROBABILITY VS. VELOCITY

BENDIX AEROSPACE SYSTEMS DIVISION-FRAGMENTATION STUDY

CHARGE WT. (#) =0.125 CASE WT. (#) =2.563 DISTANCE (METERS) =125

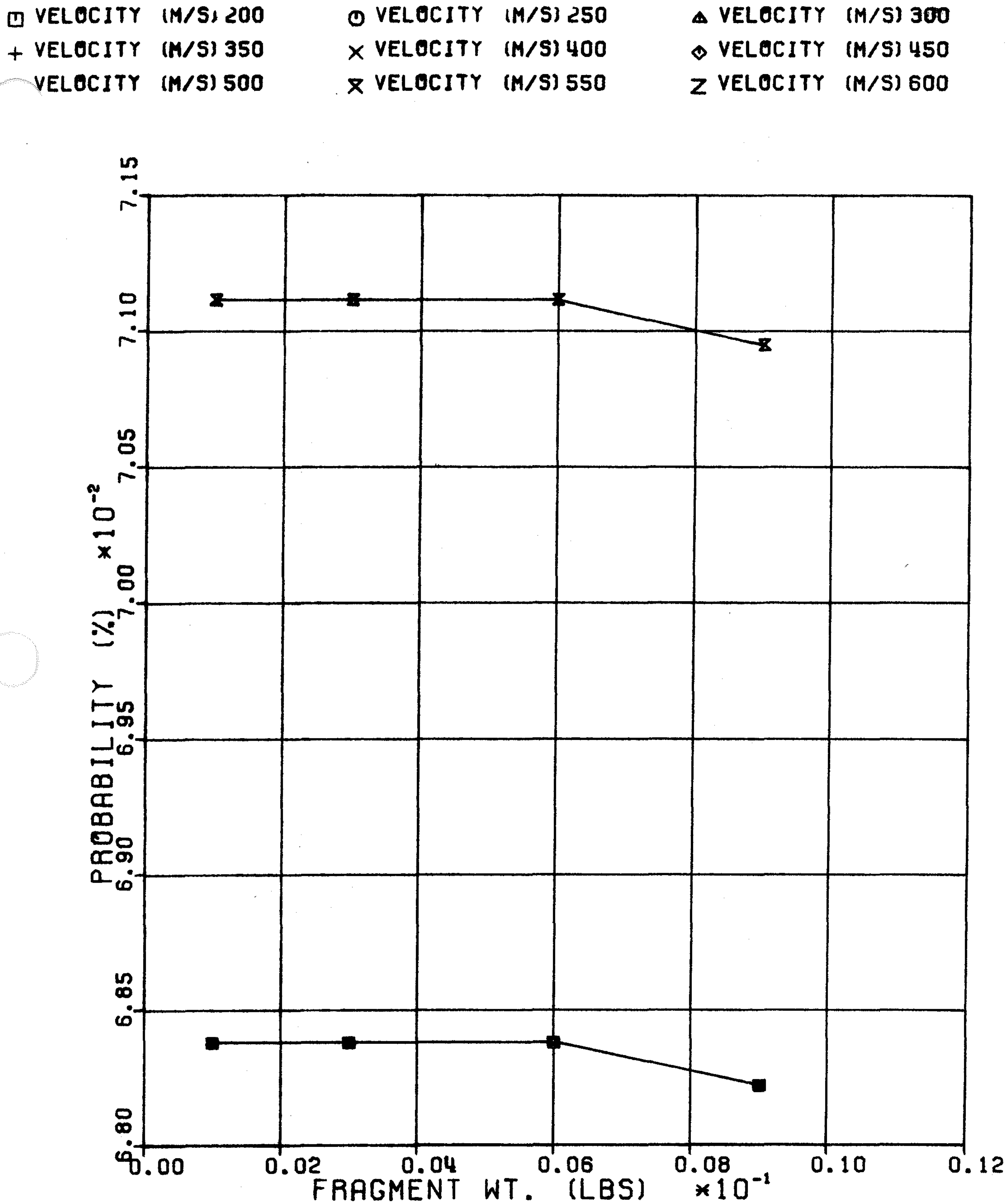

FIGURE 4 PROBABILITY OF STRIKE VS. FRAGMENT SIZE

BENDIX AEROSPACE SYSTEMS DIVISION-FRAGMENTATION STUDY

CHARGE WT. (*) =0.250 CASE WT. (*) =2.561 DISTANCE (METERS) =250

□ FRAGMENT WT. (*) =0.001 ○ FRAGMENT WT. (*) =0.003 △ FRAGMENT WT. (*) =0.006
+ FRAGMENT WT. (*) =0.009

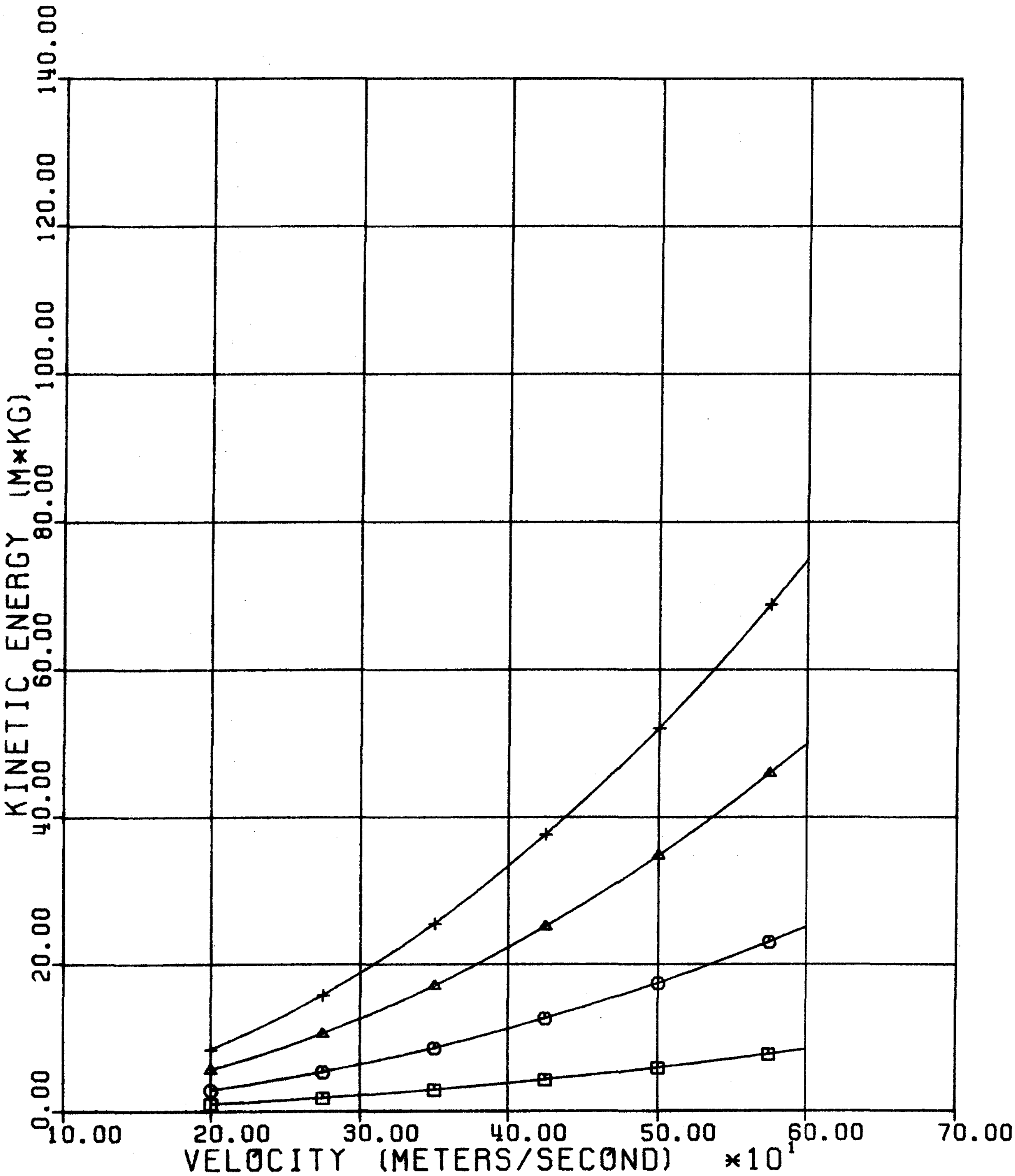

FIGURE 5 FRAGMENT K.E. VS. VELOCITY

BENDIX AEROSPACE SYSTEMS DIVISION-FRAGMENTATION STUDY

CHARGE WT. (#) =0.250 CASE WT. (#) =2.561 DISTANCE (METERS) =250

□ FRAGMENT WT. (#) =0.001 ○ FRAGMENT WT. (#) =0.003 △ FRAGMENT WT. (#) =0.006

+ FRAGMENT WT. (#) =0.009

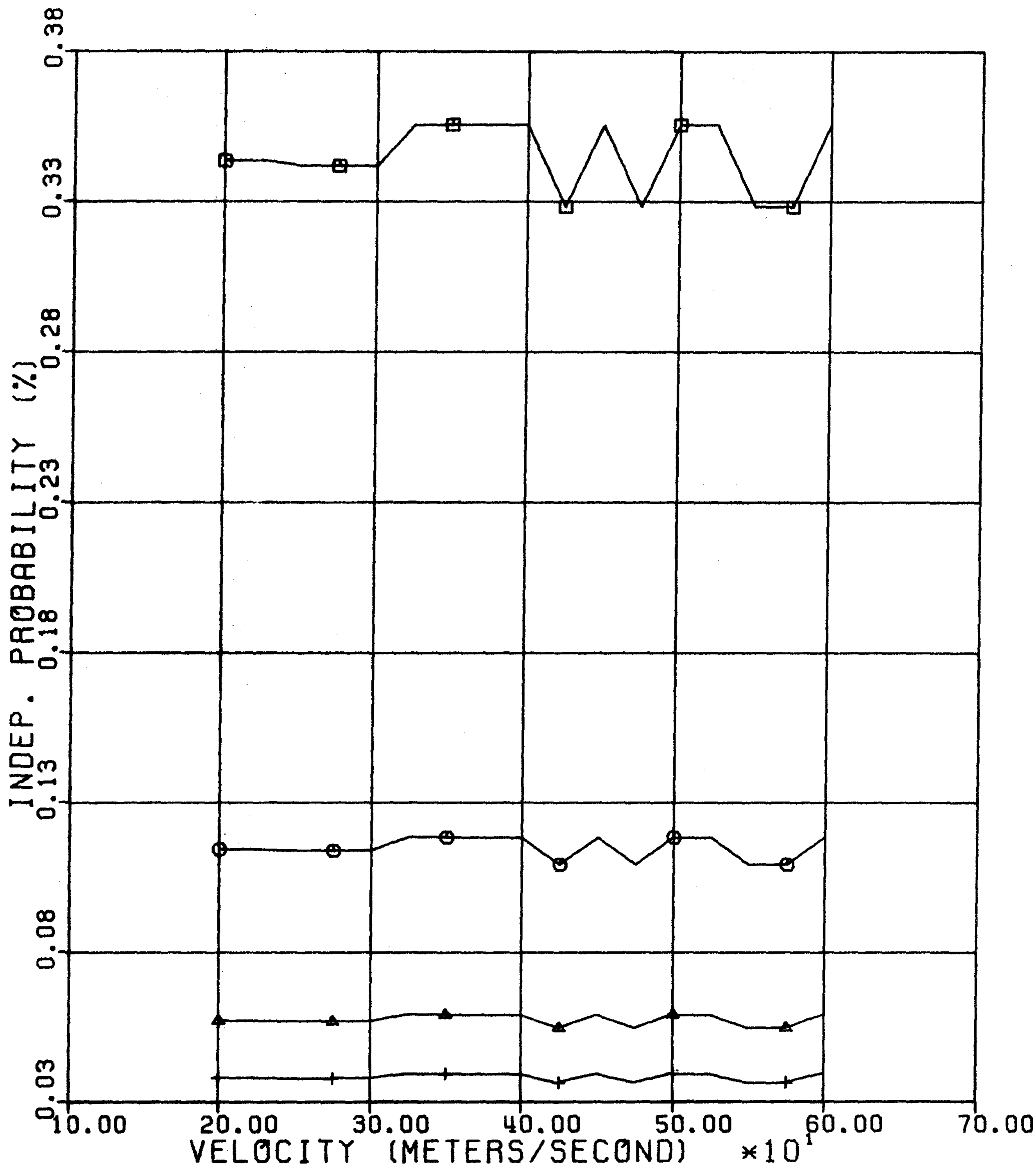

FIGURE 6 INDEPENDENT PROBABILITY VS. VELOCITY

BENDIX AEROSPACE SYSTEMS DIVISION-FRAGMENTATION STUDY

CHARGE WT. (#) =0.250   CASE WT. (#) =2.561   DISTANCE (METERS) =250

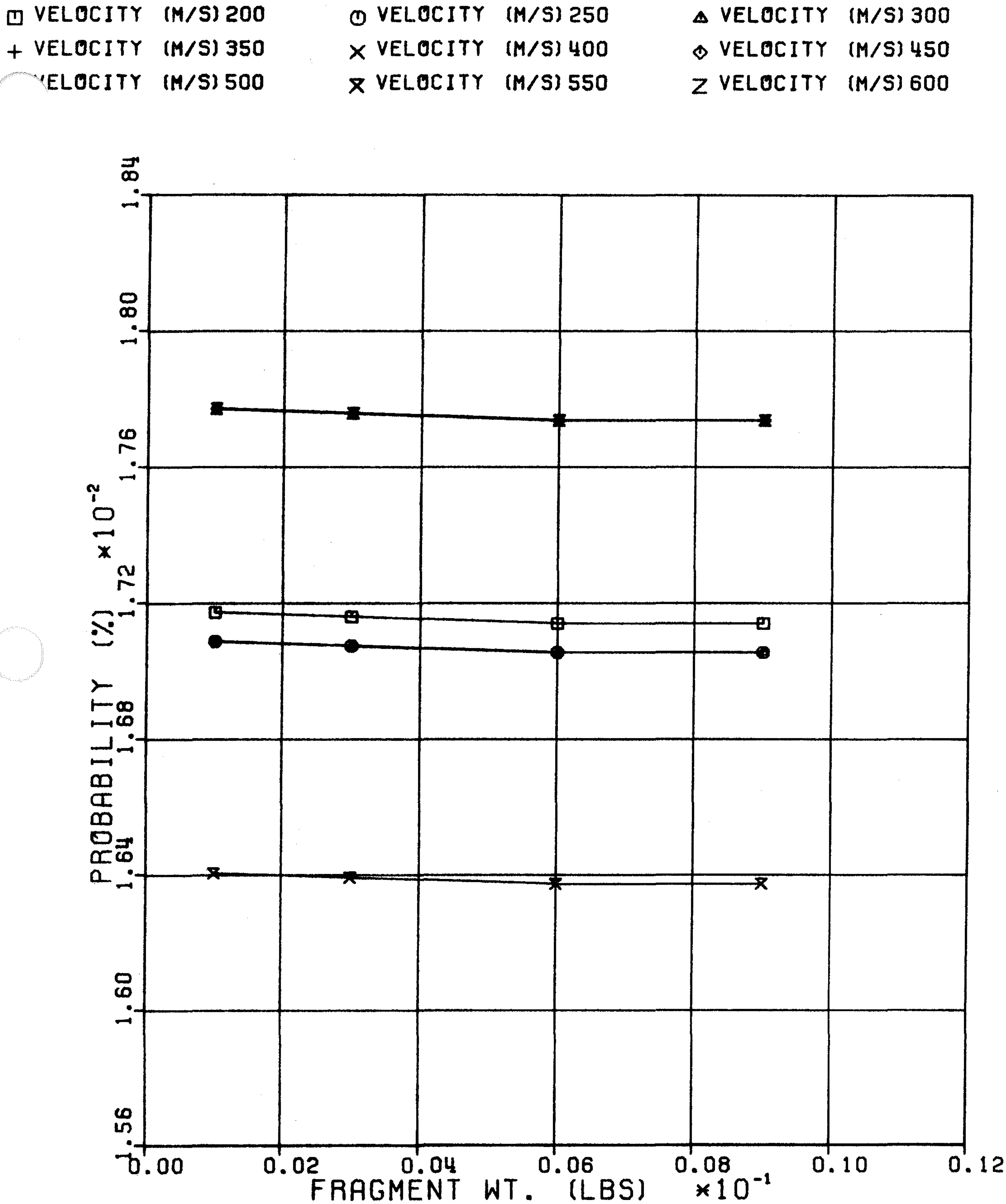

FIGURE 7 PROBABILITY OF STRIKE VS. FRAGMENT SIZE

BENDIX AEROSPACE SYSTEMS DIVISION-FRAGMENTATION STUDY

CHARGE WT. (*) =0.500 CASE WT. (*) =2.696 DISTANCE (METERS) =500

□ FRAGMENT WT. (*) =0.001 ○ FRAGMENT WT. (*) =0.003 △ FRAGMENT WT. (*) =0.006
+ FRAGMENT WT. (*) =0.009

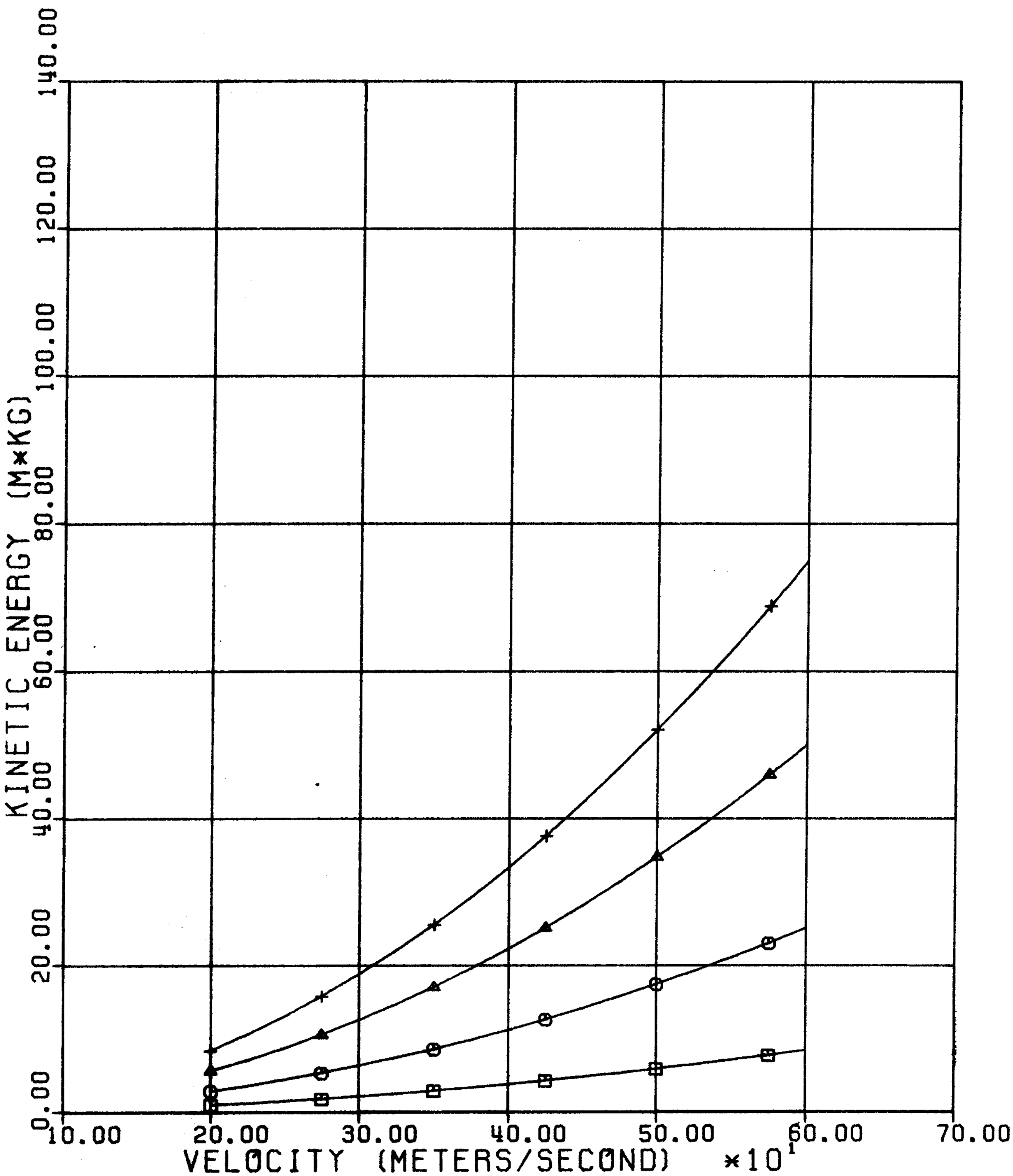

FIGURE 8 FRAGMENT K.E. VS. VELOCITY

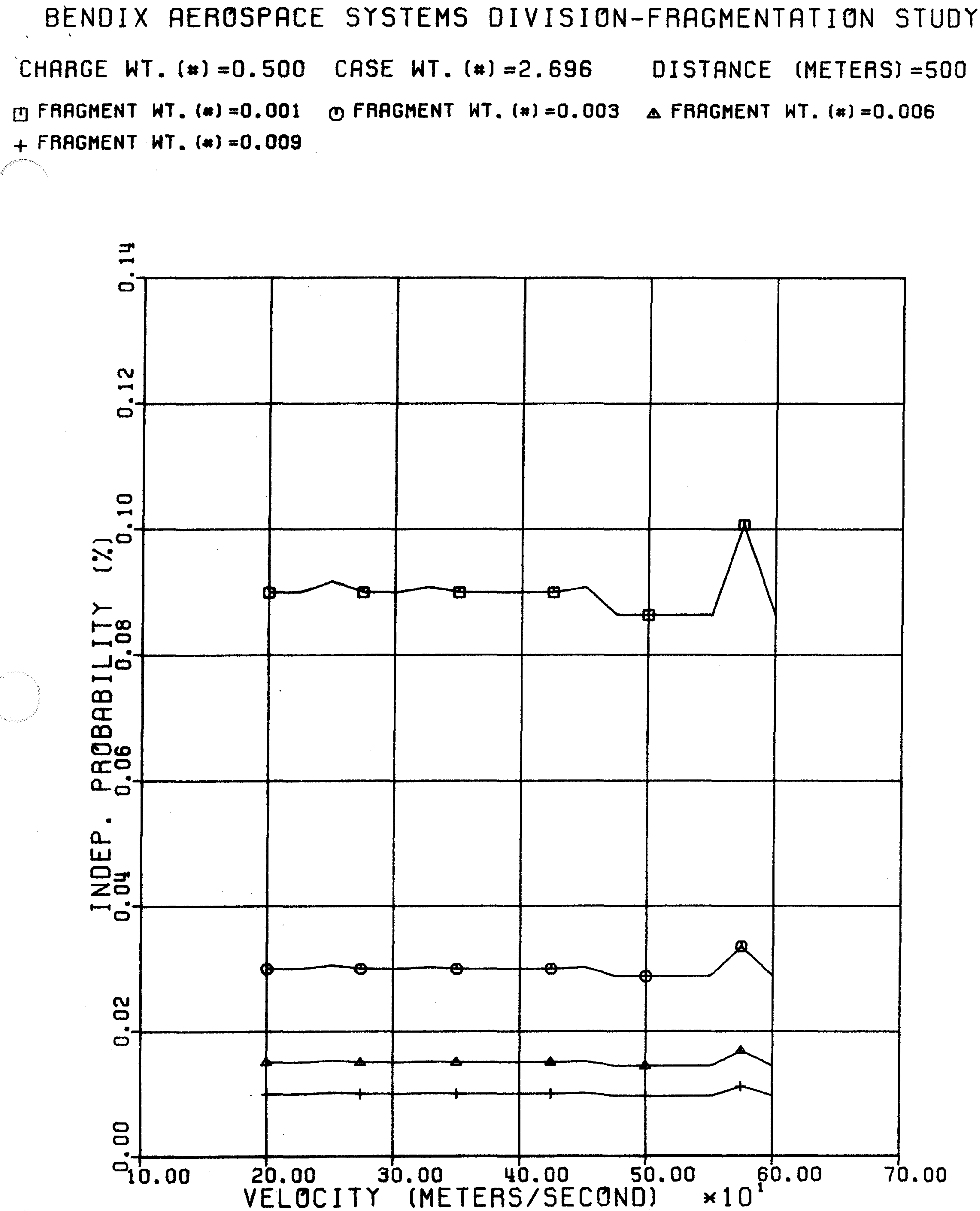

FIGURE 9 INDEPENDENT PROBABILITY VS. VELOCITY

BENDIX AEROSPACE SYSTEMS DIVISION-FRAGMENTATION STUDY

CHARGE WT. (*) =0.500 CASE WT. (*) =2.696 DISTANCE (METERS) =500

□ VELOCITY (M/S) 200 ⊙ VELOCITY (M/S) 250 △ VELOCITY (M/S) 300
+ VELOCITY (M/S) 350 × VELOCITY (M/S) 400 ◇ VELOCITY (M/S) 450
VELOCITY (M/S) 500 ⨯ VELOCITY (M/S) 550 Z VELOCITY (M/S) 600

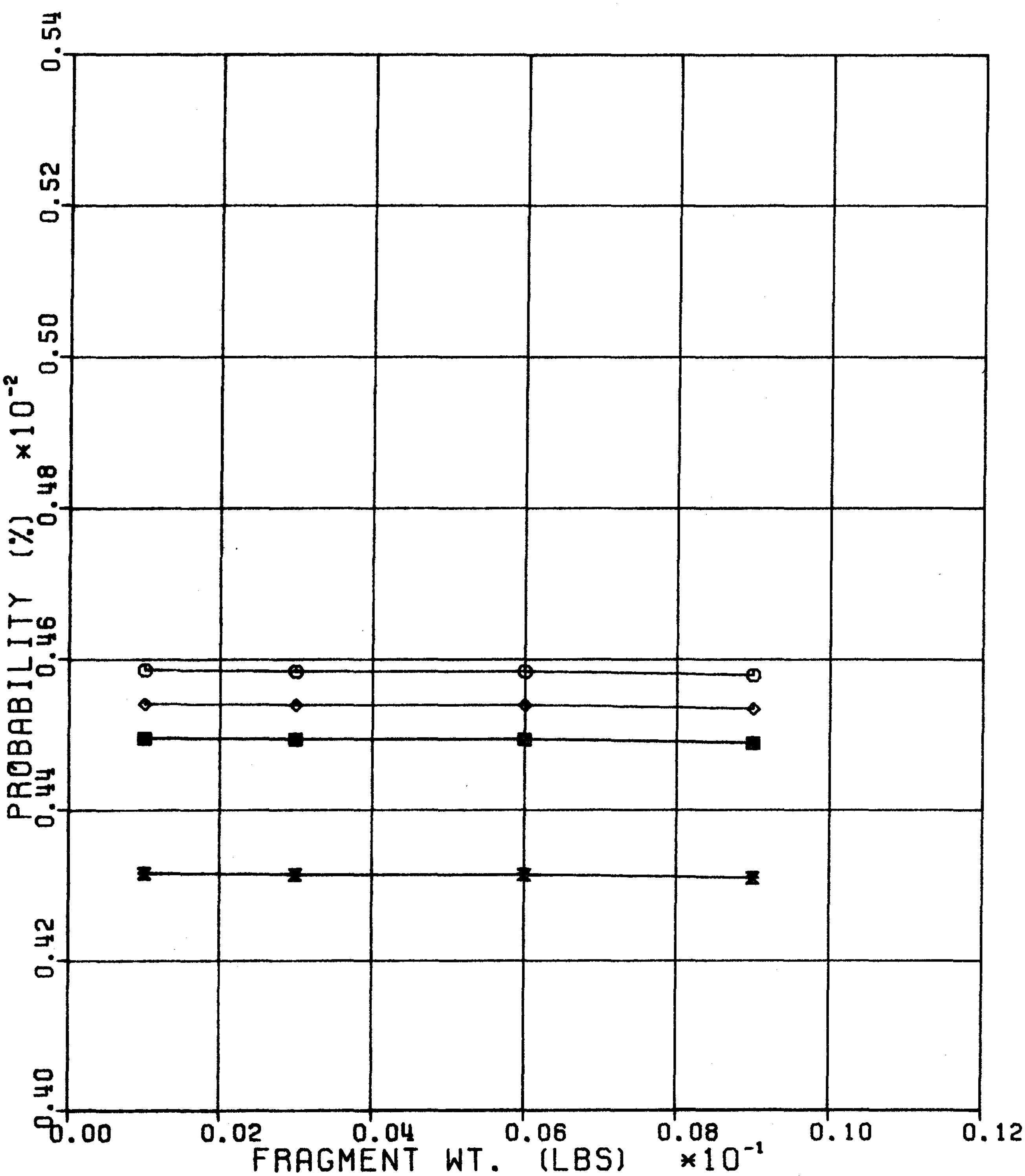

FIGURE 10 PROBABILITY OF STRIKE VS. FRAGMENT SIZE

BENDIX AEROSPACE SYSTEMS DIVISION-FRAGMENTATION STUDY

CHARGE WT. (#)=1.000 CASE WT. (#)=2.737 DISTANCE (METERS)=1000

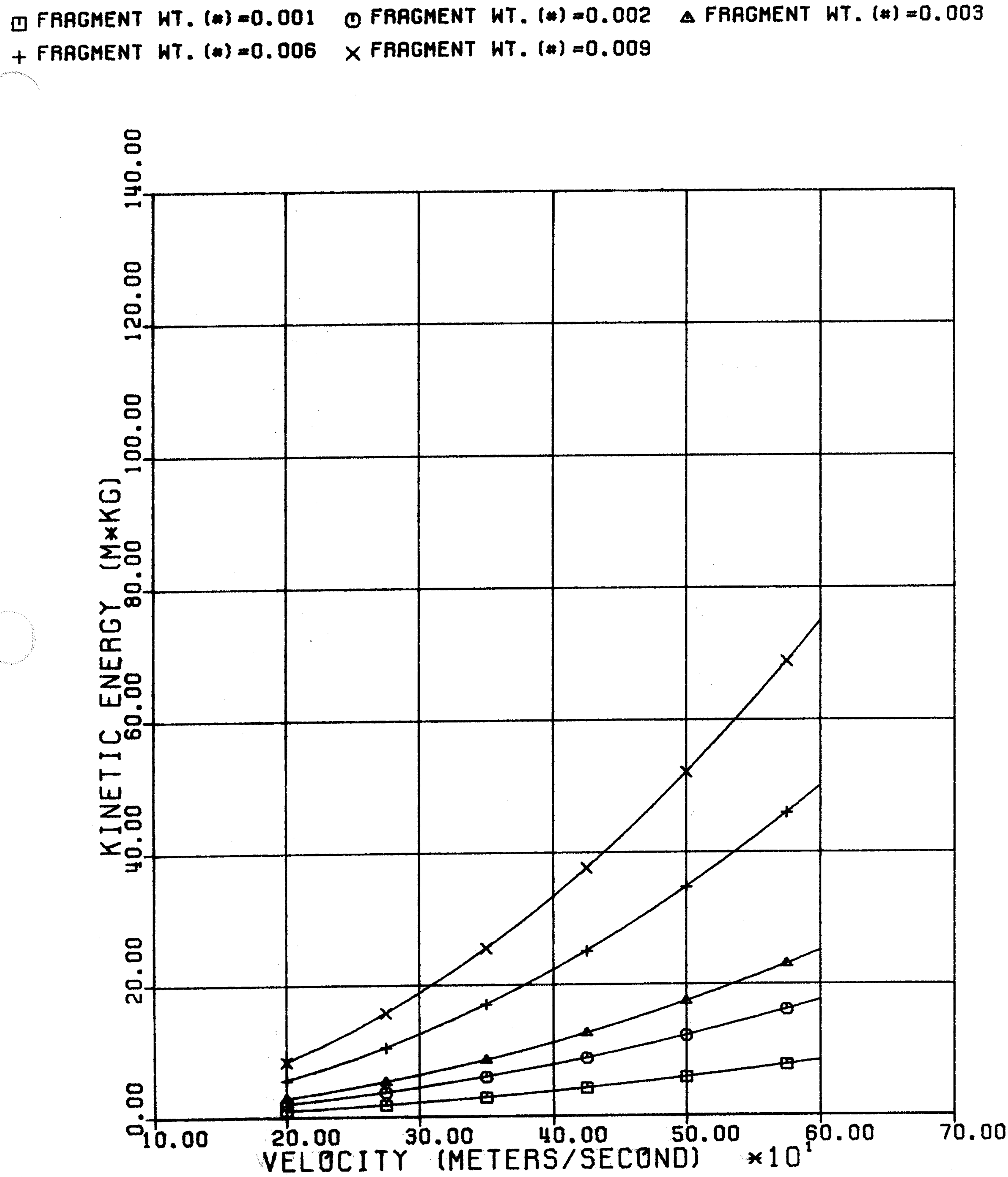

FIGURE 11 FRAGMENT K.E. VS. VELOCITY

BENDIX AEROSPACE SYSTEMS DIVISION-FRAGMENTATION STUDY

CHARGE WT. (*) =1.000 CASE WT. (*) =2.737 DISTANCE (METERS) =1000

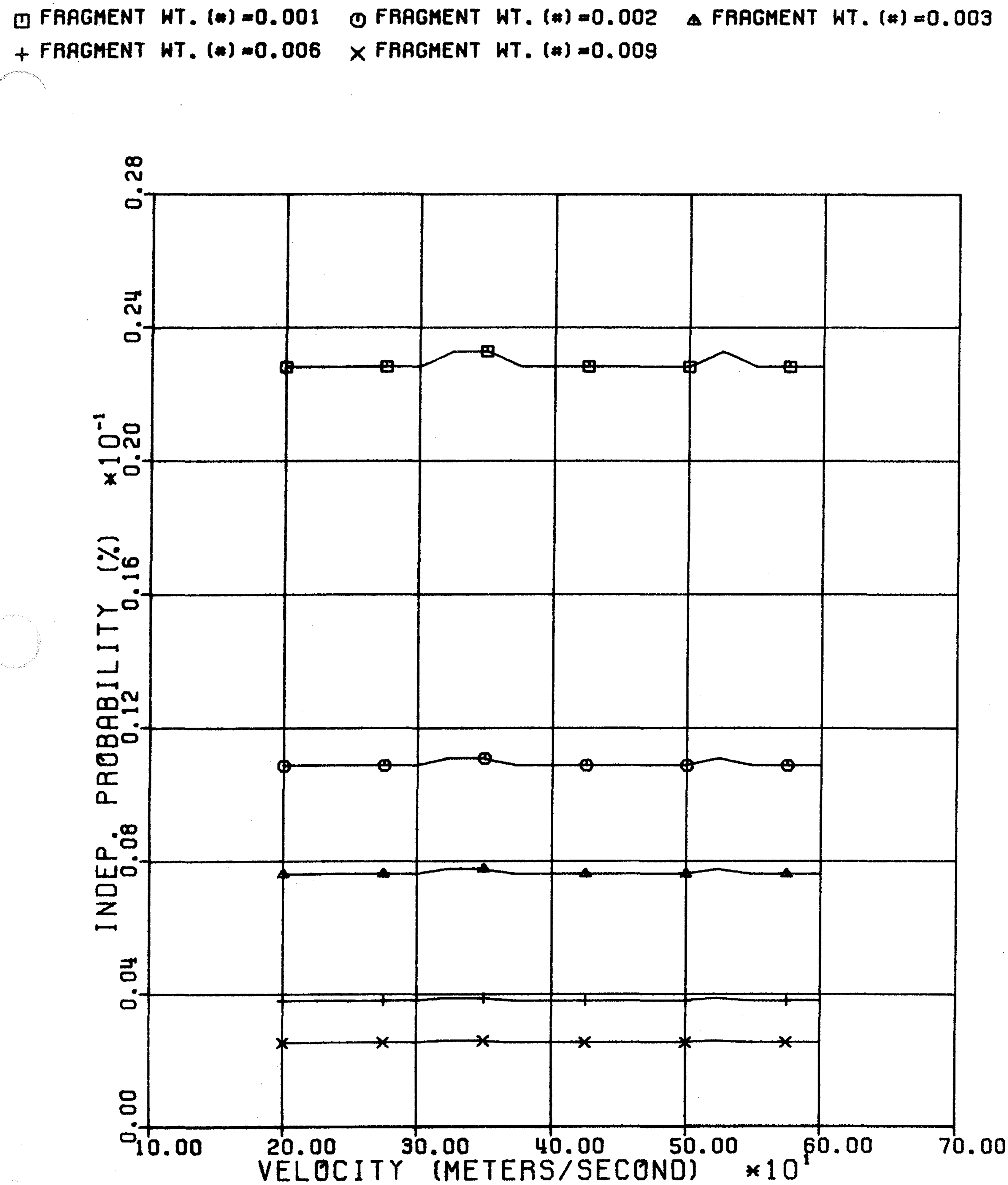

FIGURE 12 INDEPENDENT PROBABILITY VS. VELOCITY

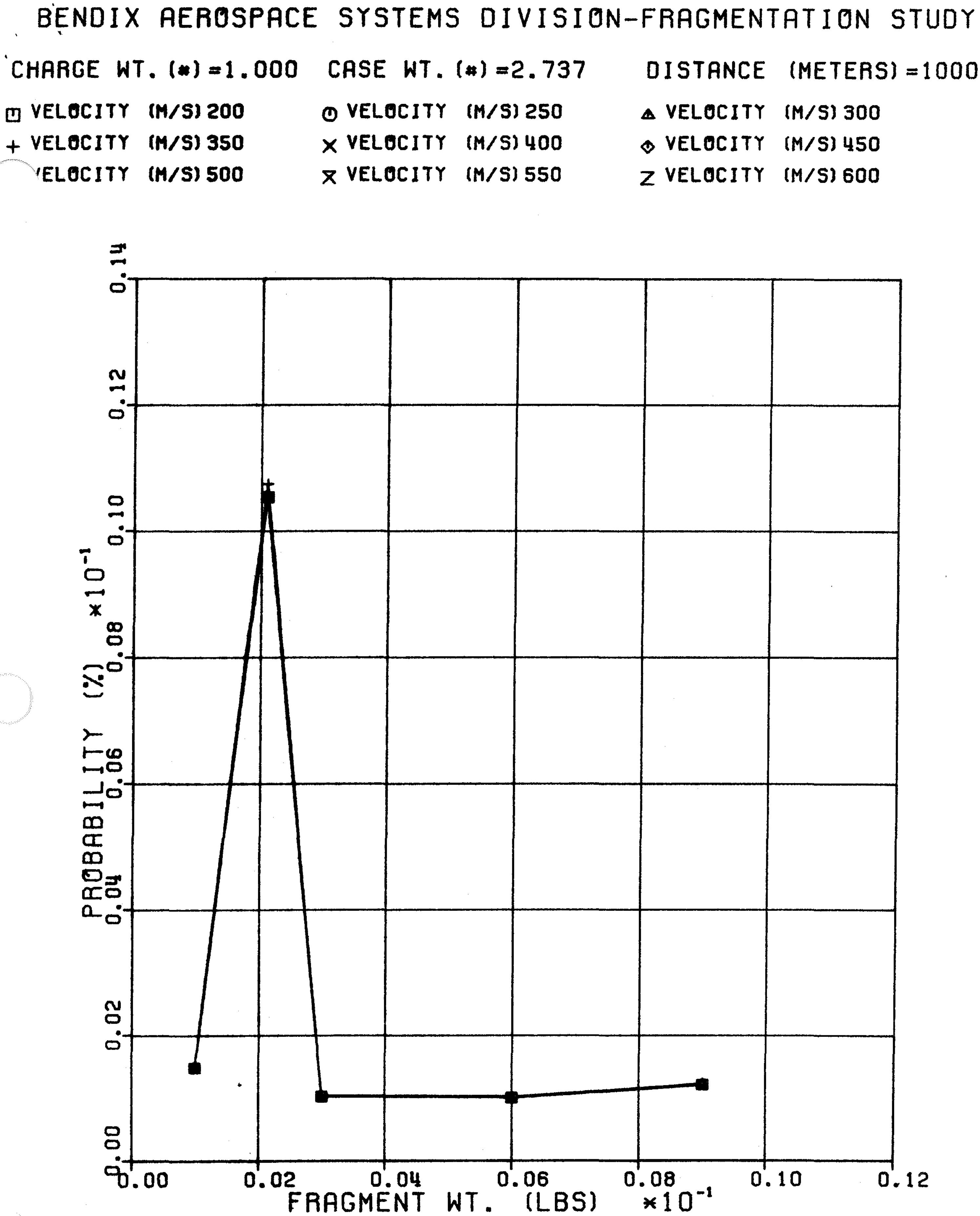

FIGURE 13 PROBABILITY OF STRIKE VS. FRAGMENT SIZE

BENDIX AEROSPACE SYSTEMS DIVISION-FRAGMENTATION STUDY

CHARGE WT. (*) =6.000 CASE WT. (*) =2.814 DISTANCE (METERS) =3500

□ FRAGMENT WT. (*) =0.001 ○ FRAGMENT WT. (*) =0.003 △ FRAGMENT WT. (*) =0.006
+ FRAGMENT WT. (*) =0.009

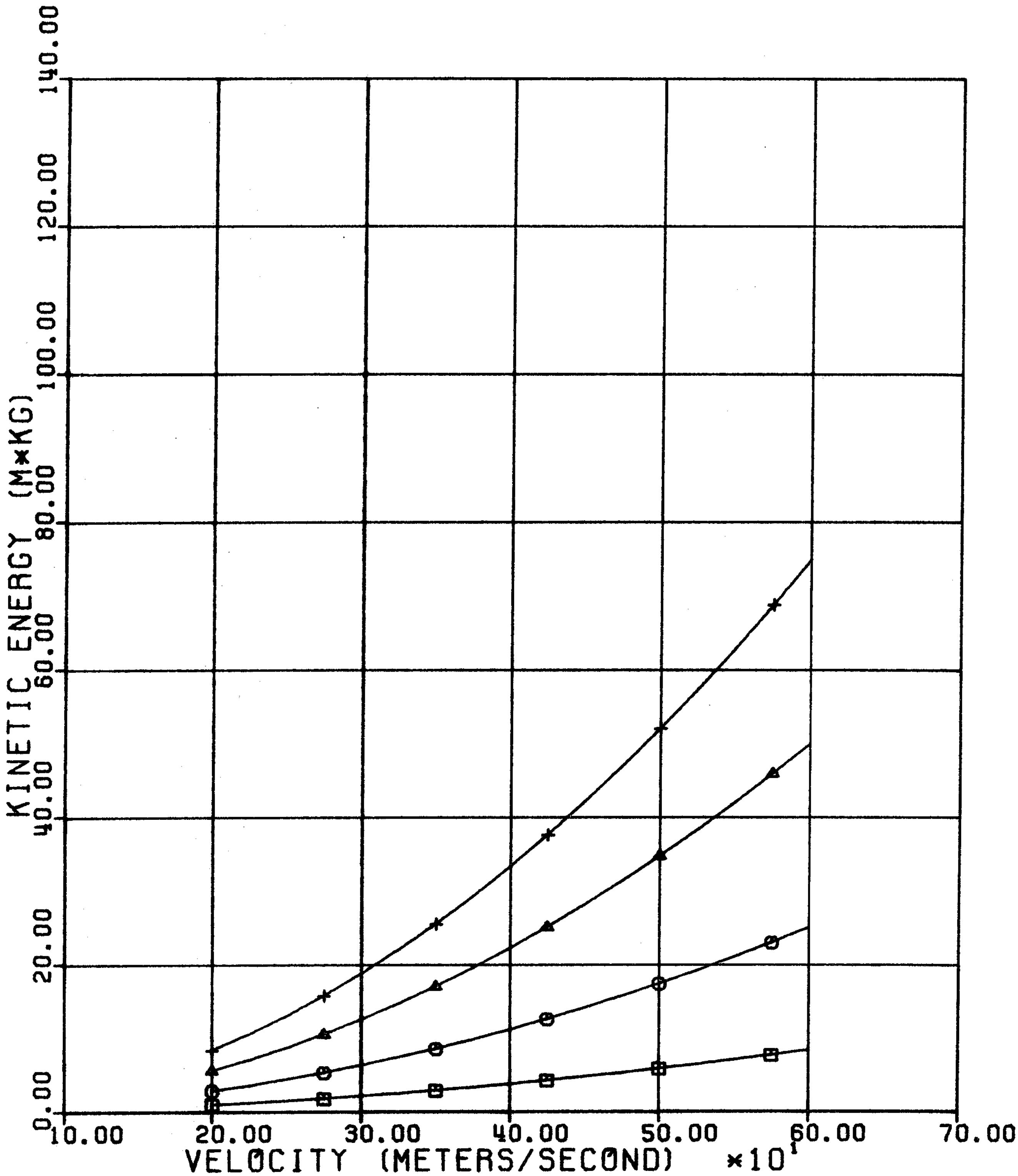

FIGURE 14 FRAGMENT K.E. VS. VELOCITY

BENDIX AEROSPACE SYSTEMS DIVISION-FRAGMENTATION STUDY

CHARGE WT. (*) =6.000 CASE WT. (*) =2.814 DISTANCE (METERS) =3500

□ FRAGMENT WT. (*) =0.001 ○ FRAGMENT WT. (*) =0.003 △ FRAGMENT WT. (*) =0.006
+ FRAGMENT WT. (*) =0.009

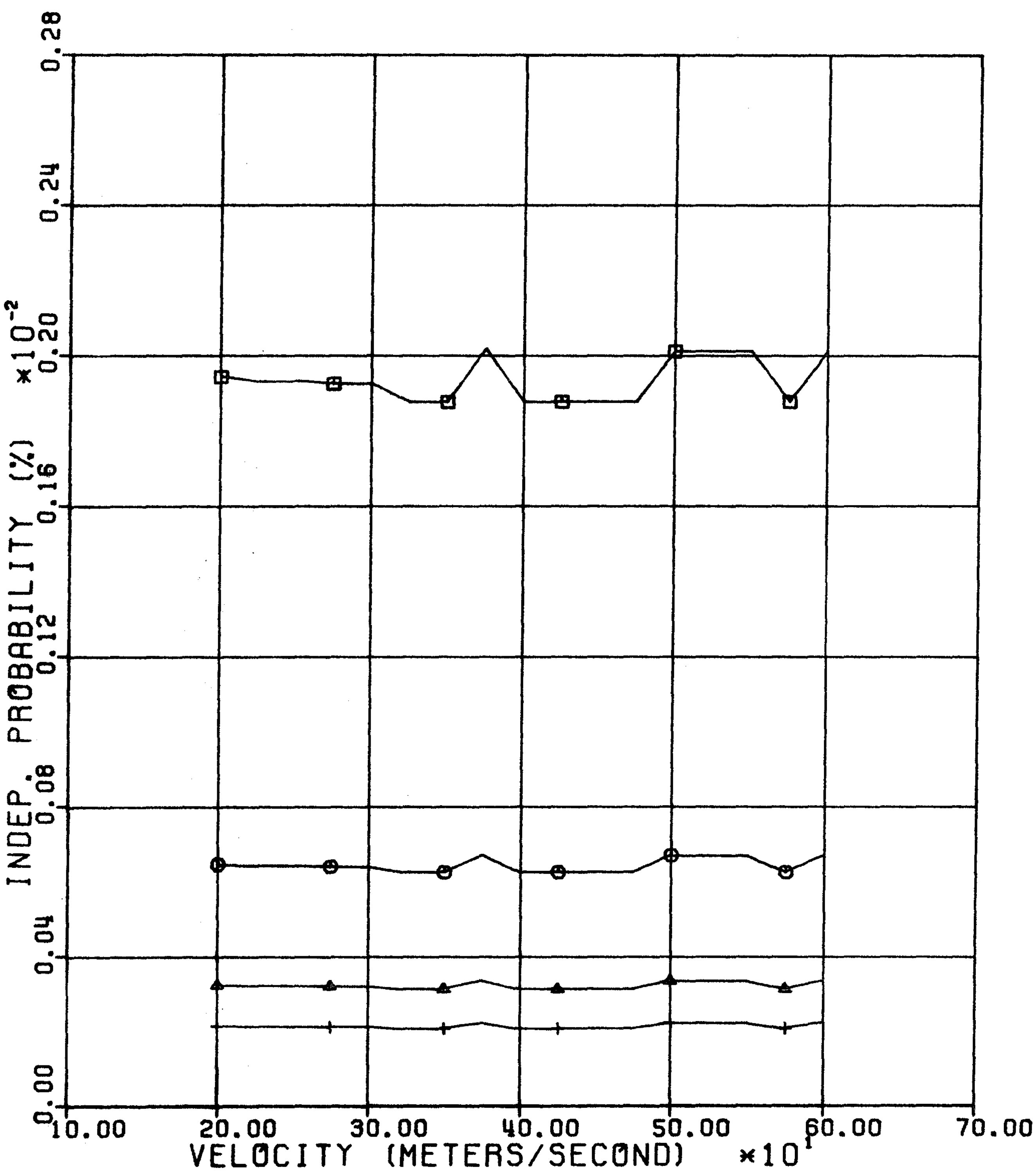

FIGURE 15 INDEPENDENT PROBABILITY VS. VELOCITY

BENDIX AEROSPACE SYSTEMS DIVISION-FRAGMENTATION STUDY

CHARGE WT. (#) =6.000 CASE WT. (#) =2.814 DISTANCE (METERS) =3500

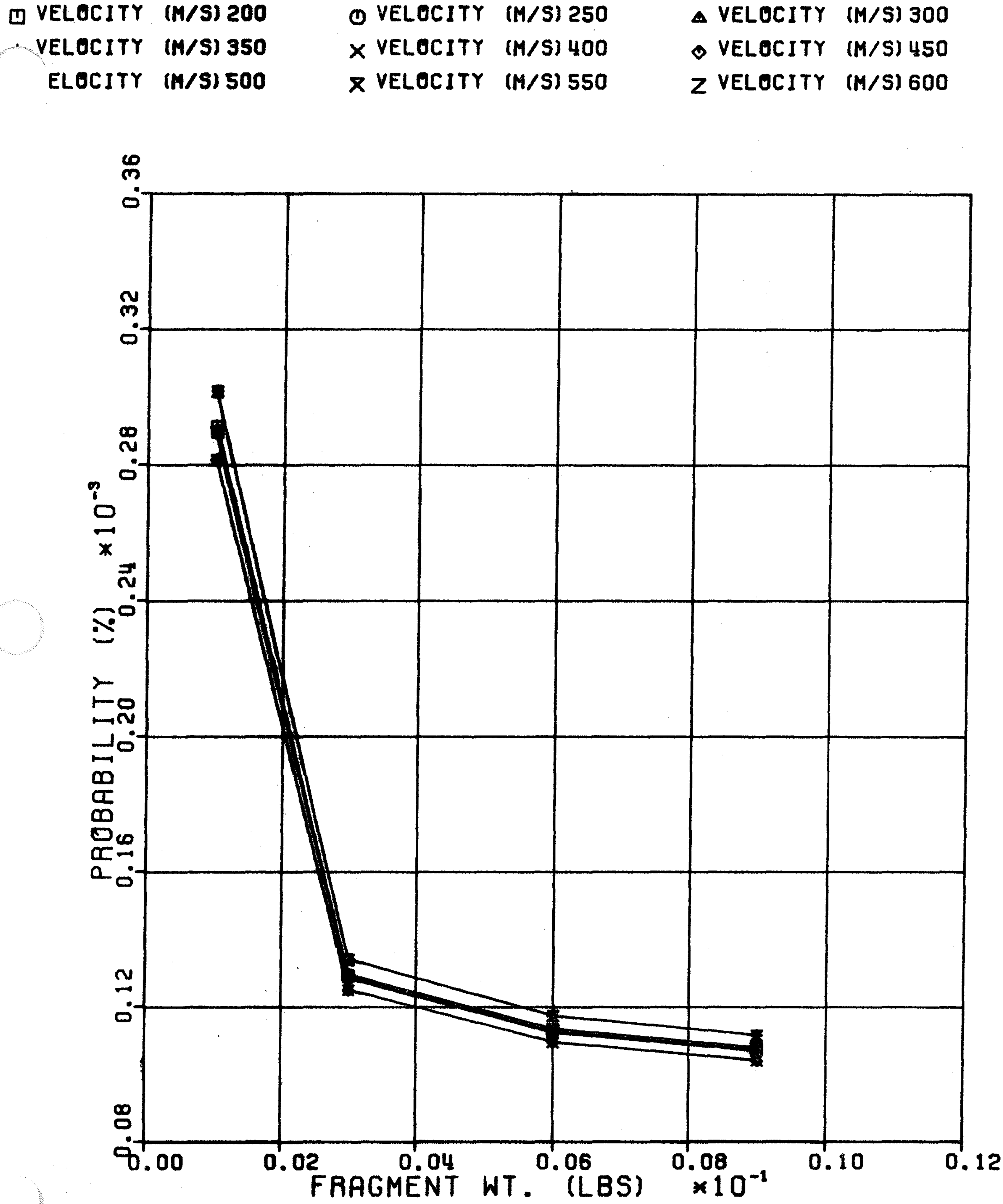

FIGURE 16 PROBABILITY OF STRIKE VS. FRAGMENT SIZE

APPENDIX

ATM 1046

```
      DIMENSION VE(20),ENGK(20),PRB(20),PR(10
      J=0
    1 READ 10,X,Y,WT,WF,PRN
   10 FORMAT (8E10.0)
      IF (X.LT.0.) GO TO 200
      J=J+1
      PRINT 2
    2 FORMAT ('1           X                Y                  WT                WF
     1     PR ON N')
      PRINT 20,X,Y,WT,WF,PRN
   20 FORMAT (5F15.6)
      NF=WT/WF
      FN=NF
      FMASS=WF*.4536/9.80665
      G=1.62
      XG=X*G
      PRH=3.54*.3048/(2.*3.1416*X)
      V=175.
      PRINT 29
   29 FORMAT ('0     VELOCITY             PHI1                PHI2          ANGLE
     1HIGH        PHJ1              PHJ2         ANGLE LOW     PROB FRAG')
      YA= 2.5*.3048
      DO 100 I=1,17
      V=V+25.
      VE(I)=V
      VSQ=V*V
      Y=0.
      B=VSQ/XG
      BSQ=B*B
      C=1.
      D=SQRT(BSQ-C)
      PHI1=ATAN(B+D)
      PHJ1=ATAN(B-D)
      Y=YA
      C=1.+2.*B*Y/X
      D=SQRT(BSQ-C)
      PHI2=ATAN(B+D)
      PHJ2=ATAN(B-D)
      AI=ABS(PHI2-PHI1)
      AJ=ABS(PHJ2-PHJ1)
      PRA=(AI+AJ)*2./3.1416
      PRINT 30,V,PHI1,PHI2,AI,PHJ1,PHJ2,AJ,PRA
   30 FORMAT (8E15.6)
      PRB(I)=PRH*PRA*FN
      PR(J,I)=PRB(I)*PRN*100.
      PRB(I)=PRB(I)*100.
      ENGK(I)=0.5*FMASS*VSQ
  100 CONTINUE
  110 PRINT 140
  140 FORMAT ('0  VELOCITY            KINETIC ENERGY   INDEP PROB          PRO
     1BABILITY')
      PUNCH 145,J
      PUNCH 146,WF
      DO 120 I=1,17
      PUNCH 160,VE(I),ENGK(I),PRB(I),PR(J,I)
  120 PRINT 130,VE(I),ENGK(I),PRB(I),PR(J,I)
  145 FORMAT (I5)
  146 FORMAT (F10.4)
```

APPENDIX -- TRAJECTORY AND PROBABILITY PROGRAM LISTING AND PLOT ROUTINE

```
  160 FORMAT (4E15.6)
  130 FORMAT ( 4(E15.6,2X))
      GO TO 1
  200 STOP
      END
```

ATM 1046

ATM 1046

```
      DIMENSION BUFF(1024),WORDA(20),WORDB([illegible]ORDC(20),VE(20),EV(20)
      DIMENSION ENGK(20,10),PRB(20,10),PR([illegible]ARRAYE(4),WF(10)
      M=1
      READ 5,WORDA
      READ 5,WORDB
      READ 5,WORDC
    5 FORMAT (20A4)
      READ 8,WCR,WCS,DIST
    8 FORMAT (3E10.0)
    2 READ 10,J
   10 FORMAT (I5)
      IF (J.EQ.-1) GO TO 30
      READ 7,WF(J)
    7 FORMAT (E10.0)
      DO 20 I=1,17
   20 READ 15,VE(I),ENGK(I,J),PRB(I,J),PR(J,I)
   15 FORMAT (4E15.6)
      JJ=J
      GO TO 2
   30 ARRAYE(1)=ENGK(1,1)
      ARRAYE(2)=ENGK(1,1)
      DO 40 J=1,JJ
      DO 40 I=1,17
      IF (ARRAYE(1).LT.ENGK(I,J)) ARRAYE(1)=ENGK(I,J)
   40 IF (ARRAYE(2).GT.ENGK(I,J)) ARRAYE(2)=ENGK(I,J)
      CALL PLOTS (BUFF,1024,11)
      CALL PLOT (20.,-30.5,-3)
      CALL AXIS (1.5,1.5,'VELOCITY (METERS/SECOND)',-24,6.,0.,100.,100.)
      CALL SYMBOL (0.6,0.5,.14,'FIGURE',0.0,6)
      CALL SYMBOL (2.0,0.5,.14,WORDA,0.0,80)
      CALL SCALE (ARRAYE,7.0,2,1)
      CALL AXIS (1.5,1.5,'KINETIC ENERGY (M*KG)',21,7.,90.,ARRAYE(3),
     1ARRAYE(4))
      VE(18)=100.0
      VE(19)=100.0
      EV(18)=ARRAYE(3)
      EV(19)=ARRAYE(4)
      PRINT 6,WORDA
    6 FORMAT ('1',20A4)
   35 CALL GRID (1.5,1.5,1.0,1.0,6,7)
      CALL SYMBOL (0.7,10.5,0.14,'BENDIX AEROSPACE SYSTEMS DIVISION-FRAG
     1MENTATION STUDY',0.0,53)
      CALL SYMBOL (0.5,10.10,0.12,'CHARGE WT.(#)=',0.0,14)
      CALL NUMBER (999.,999.,0.12,WCR,0.0,3)
      CALL SYMBOL (3.0,10.10,0.12,'CASE WT.(#)=',0.0,12)
      CALL NUMBER (999.,999.,0.12,WCS,0.0,3)
      CALL SYMBOL (5.5,10.10,0.12,'DISTANCE (METERS)=',0.0,18)
      CALL NUMBER (999.,999.,0.12,DIST,0.0,-1)
      CALL PLOT (1.5,1.5,-3)
      DO 90 J=1,JJ
      INTEQ=J-1
      DO 47 I=1,17
      IF (M.EQ.1) EV(I)=ENGK(I,J)
      IF (M.EQ.2) EV(I)=PRB(I,J)
   47 CONTINUE
      GO TO (70,71,72,73,74,75,76,77,78,79,80,81,82,83),J
   70 CALL SYMBOL (-1.0,8.30,0.10,00,0.0,-1)
      GO TO 84
```

(4)


```
0057      71 CALL SYMBOL (1.50,8.30,0.10,01,0.0,-1)
0058         GO TO E4
0059      72 CALL SYMBOL (4.00,8.30,0.10,02,0.0,-1)
0060         GO TO E4
0061      73 CALL SYMBOL (-1.0,8.05,0.10,03,0.0,-1)
0062         GO TO E4
0063      74 CALL SYMBOL (1.50,8.05,0.10,04,0.0,-1)
0064         GO TO E4
0065      75 CALL SYMBOL (4.00,8.05,0.10,05,0.0,-1)
0066         GO TO E4
0067      76 CALL SYMBOL (-1.0,7.80,0.10,06,0.0,-1)
0068         GO TO E4
0069      77 CALL SYMBOL (1.50,7.80,0.10,07,0.0,-1)
0070         GO TO E4
0071      78 CALL SYMBOL (4.00,7.80,0.10,08,0.0,-1)
0072         GO TO E4
0073      79 CALL SYMBOL (-1.0,7.55,0.10,09,0.0,-1)
0074         GO TO E4
0075      80 CALL SYMBOL (1.50,7.55,0.10,10,0.0,-1)
0076         GO TO E4
0077      81 CALL SYMBOL (4.00,7.55,0.10,11,0.0,-1)
0078         GO TO E4
0079      82 CALL SYMBOL (-1.0,7.30,0.10,12,0.0,-1)
0080         GO TO E4
0081      83 CALL SYMBOL (1.50,7.30,0.10,13,0.0,-1)
0082      84 CALL SYMBOL (999.,999.,0.1,'FRAGMENT WT.(#)=',0.0,16)
0083         CALL NUMBER (999.,999.,0.1,WF(J),0.0,3)
0084         CALL LINE (VE,EV,17,1,3,INTEQ)
0085      90 CONTINUE
0086         M=M+1
0087         CALL PLOT (15.,-30.5,-3)
0088         IF (M-3) 91,93,150
0089      91 CALL AXIS (1.5,1.5,'VELOCITY (METERS/SECOND)',-24,6.,0.,100.,100.)
0090         CALL SYMBOL (0.6,0.5,.14,'FIGURE',0.0,6)
0091         CALL SYMBOL (2.0,0.5,.14,WORDB,0.0,80)
0092         ARRAYE(1)=PRB(1,1)
0093         ARRAYE(2)=PRB(1,1)
0094         DO 92 J=1,JJ
0095         DO 92 I=1,17
0096         IF (ARRAYE(1).LT. PRB(I,J)) ARRAYE(1)=PRB(I,J)
0097      92 IF (ARRAYE(2).GT. PRB(I,J)) ARRAYE(2)=PRB(I,J)
0098         CALL SCALE (ARRAYE,7.0,2,1)
0099         EV(18)=ARRAYE(3)
0100         EV(19)=ARRAYE(4)
0101         CALL AXIS (1.5,1.5,'INDEP. PROBABILITY (%)',22,7.0,90.0,ARRAYE(3),
            1ARRAYE(4))
0102         PRINT 6,WORDB
0103         GO TO 35
0104      93 DO 94 I=1,20
0105      94 EV(I)=0.0
0106         CALL AXIS (1.5,1.5,'FRAGMENT WT. (LBS)',-18,6.0,0.,0.,.002)
0107         CALL SYMBOL (0.6,0.5,.14,'FIGURE',0.0,6)
0108         CALL SYMBOL (2.0,0.5,.14,WORDC,0.0,80)
0109         ARRAYE(1)=PR(1,1)
0110         ARRAYE(2)=PR(1,1)
0111         DO 100 I=1,17
0112         DO 100 J=1,JJ
0113         IF (ARRAYE(1).LT.PR(J,I)) ARRAYE(1)=PR(J,I)
```

ATM 1046

```
  100 IF (ARRAYE(2).GT.PR(J,I)) ARRAYE(2)=PR(J,I)
      CALL SCALE (ARRAYE,7.0,2,1)
      EV(JJ+1)=ARRAYE(3)
      EV(JJ+2)=ARRAYE(4)
      CALL AXIS (1.5,1.5,'PROBABILITY (%)',15,7.0,90.,ARRAYE(3),
     1ARRAYE(4))
      WF(JJ+1)=0.0
      WF(JJ+2)=0.002
      PRINT 6,WORDC
      CALL GRID (1.5,1.5,1.0,1.0,6,7)
      CALL SYMBOL (C.7,10.5,0.14,'BENDIX AERCSPACE SYSTEMS DIVISION-FRAG
     1MENTATION STUDY',C.0,53)
      CALL SYMBOL (0.5,10.10,0.12,'CHARGE WT.(#)=',0.0,14)
      CALL NUMBER (999.,999.,0.12,WCR,0.0,3)
      CALL SYMBOL (3.0,10.10,0.12,'CASE WT.(#)=',0.0,12)
      CALL NUMBER (999.,999.,0.12,WCS,0.0,3)
      CALL SYMBOL (5.5,10.10,0.12,'DISTANCE (METERS)=',0.0,18)
      CALL NUMBER (999.,999.,0.12,DIST,0.0,-1)
      CALL PLOT (1.5,1.5,-3)
  111 DO 19C I=1,17,2
      DO 16C J=1,JJ
  160 EV(J)=PR(J,I)
      II=1
      IF (I.NE.1) II=I/2+1
      GO TO (50,51,52,53,54,55,56,57,58,59,60,61,62,63),II
   50 CALL SYMBOL (-1.0,8.30,0.10,00,0.0,-1)
      GO TO €4
   51 CALL SYMBOL (1.50,8.30,0.10,01,0.0,-1)
      GO TO €4
   52 CALL SYMBOL (4.00,8.30,0.1C,02,0.0,-1)
      GO TO €4
   53 CALL SYMBOL (-1.0,8.05,0.10,03,0.0,-1)
      GO TO €4
   54 CALL SYMBOL (1.50,8.05,0.10,04,0.0,-1)
      GO TO €4
   55 CALL SYMBOL (4.00,8.05,0.10,05,0.0,-1)
      GO TO €4
   56 CALL SYMBOL (-1.0,7.80,0.10,06,0.0,-1)
      GO TO €4
   57 CALL SYMBOL (1.50,7.80,0.10,07,0.0,-1)
      GO TO €4
   58 CALL SYMBOL (4.00,7.80,0.10,08,0.0,-1)
      GO TO €4
   59 CALL SYMBOL (-1.0,7.55,0.1C,09,0.0,-1)
      GO TO €4
   60 CALL SYMBOL (1.50,7.55,0.10,10,0.0,-1)
      GO TO €4
   61 CALL SYMBOL (4.00,7.55,0.10,11,0.0,-1)
      GO TO €4
   62 CALL SYMBOL (-1.0,7.30,0.1C,12,0.0,-1)
      GO TO €4
   €3 CALL SYMBOL (1.50,7.30,0.10,13,0.0,-1)
   €4 CALL SYMBOL (999.,999.,0.1,'VELOCITY (M/S)',0.0,14)
      CALL NUMBER (999.,999.,0.1,VE(I),0.,-1)
      INTEQ=II-1
      CALL LINE (WF,EV,JJ,1,1,INTEQ)
  190 CONTINUE
  150 CALL PLOT (15.,-3C.,999)
```

ATM 1046

```
0170          STOP
0171          END
```

ATM 1046